DOI: 10.1534/genetics.104.036905

The Absence of Top3 Reveals an Interaction Between the Sgs1 and Pif1 DNA Helicases in *Saccharomyces cerevisiae*

Marisa Wagner, Gavrielle Price and Rodney Rothstein[1]

Department of Genetics and Development, College of Physicians and Surgeons, Columbia University, New York, New York 10032-2704

Manuscript received September 27, 2004
Accepted for publication June 30, 2006

ABSTRACT

RecQ DNA helicases and Topo III topoisomerases have conserved genetic, physical, and functional interactions that are consistent with a model in which RecQ creates a recombination-dependent substrate that is resolved by Topo III. The phenotype associated with Topo III loss suggests that accumulation of a RecQ-created substrate is detrimental. In yeast, mutation of the *TOP3* gene encoding Topo III causes pleiotropic defects that are suppressed by deletion of the RecQ homolog Sgs1. We searched for gene dosage suppressors of *top3* and identified Pif1, a DNA helicase that acts with polarity opposite to that of Sgs1. Pif1 overexpression suppresses multiple *top3* defects, but exacerbates *sgs1* and *sgs1 top3* defects. Furthermore, Pif1 helicase activity is essential in the absence of Top3 in an Sgs1-dependent manner. These data clearly demonstrate that Pif1 helicase activity is required to counteract Sgs1 helicase activity that has become uncoupled from Top3. Pif1 genetic interactions with the Sgs1–Top3 pathway are dependent upon homologous recombination. We also find that Pif1 is recruited to DNA repair foci and that the frequency of these foci is significantly increased in *top3* mutants. Our results support a model in which Pif1 has a direct role in the prevention or repair of Sgs1-induced DNA damage that accumulates in *top3* mutants.

DNA helicases and topoisomerases represent two classes of enzymes that are important for maintaining the fidelity of genetic information after DNA damage and during chromosome replication and segregation. A combined helicase–topoisomerase activity has been evolutionarily conserved across many species (Duguet 1997; Wu *et al.* 1999). These activities exist in a single polypeptide in reverse gyrase, an enzyme that is unique to archaebacteria (Declais *et al.* 2000; Duguet *et al.* 2001). In eubacteria and in eukaryotes ranging from yeast to humans, two separate protein families, RecQ DNA helicases and DNA topoisomerases, specifically Topoisomerase III-like members, exhibit genetic and physical interactions consistent with a conserved RecQ–Topo III protein complex (reviewed in Bachrati and Hickson 2003).

The RecQ DNA helicase family, named for the prototypical member from *Escherichia coli*, includes Sgs1 from *Saccharomyces cerevisiae*, Rqh1 from *Schizosaccharomyces pombe*, and Blm, Wrn, RecQL, RecQL4, and RecQL5 from humans (Gangloff *et al.* 1994b; Murray *et al.* 1997; Stewart *et al.* 1997; Aravind *et al.* 1999; Bachrati and Hickson 2003). Multiple lines of evidence suggest a role for RecQ during homologous recombination. In all species studied, mutation of a RecQ homolog results in hyperrecombination and genome instability. In humans, mutations in Blm, Wrn, and RecQL4 cause the genetic disorders Bloom, Werner, and Rothmund–Thomson, respectively, which are characterized by an increased predisposition to cancer (reviewed in Bachrati and Hickson 2003). *In vitro*, RecQ DNA helicases unwind duplex DNA in a 3′ to 5′ direction with a marked preference for forked DNA substrates and can disrupt joint DNA molecules via branch migration (Bennett *et al.* 1998, 1999; Harmon and Kowalczykowski 1998; Constantinou *et al.* 2000; Karow *et al.* 2000). Sgs1 and Blm physically interact with the DNA strand exchange protein Rad51 in their respective organisms, pointing to an intimate relationship between RecQ and homologous recombination machinery (Wu *et al.* 2001). Furthermore, defects in both *S. pombe* cells that lack Rqh1 and mammalian cells that lack Wrn are suppressed by heterologous expression of a bacterial Holliday junction resolvase, indicating that recombination intermediates accumulate in the absence of RecQ (Doe *et al.* 2000; Saintigny *et al.* 2002).

Topoisomerase III was first identified in *S. cerevisiae* because mutations in the *TOP3* gene cause hyperrecombination (Wallis *et al.* 1989). Loss of Topo III function in *E. coli* similarly causes genomic instability (Schofield *et al.* 1992) and Topo III is essential in fission yeast (Goodwin *et al.* 1999; Maftahi *et al.* 1999). There are two mammalian isoforms. In mice, Topo IIIα deficiency is embryonic lethal while Topo IIIβ deficiency causes multiple organ defects and reduced life span (Li and Wang 1998; Kwan and Wang 2001). Topo

[1]*Corresponding author:* Department of Genetics and Development, Columbia University Medical Center, 701 W. 168th St., New York, NY 10032-2704. Email: rothstein@cancercenter.columbia.edu

III belongs to the type 1A subfamily of topoisomerases whose members catalyze ssDNA passage events and are characterized by the ability to relax negatively supercoiled DNA (Champoux 2001). However, *in vitro* and *in vivo* evidence indicate that Topo III does not efficiently remove negative supercoils, raising the possibility that it is not a typical topoisomerase (DiGate and Marians 1988; Wallis *et al.* 1989; Kim and Wang 1992).

The first clues that RecQ helicases and Topo III function together came from studies in *S. cerevisiae*. Mutant *top3* yeast cells exhibit pleiotropic defects that include slow growth accompanied by the accumulation of cells in G2/M, increased recombination between direct repeats, chromosome segregation defects, meiotic failure, and hypersensitivity to agents that create DNA lesions or arrest DNA replication (Wallis *et al.* 1989 ; Gangloff *et al.* 1994b; Chakraverty *et al.* 2001). Mutations in the *SGS1* gene were identified as suppressors of *top3* mutant slow growth (Gangloff *et al.* 1994b). An *sgs1* mutation by itself causes pleiotropic defects reminiscent of the *top3* phenotype, albeit milder in severity (Gangloff *et al.* 1994b; Watt *et al.* 1995). Epistasis analysis indicates that Sgs1 functions upstream of Top3 and the two proteins physically interact (Gangloff *et al.* 1994b; Bennett *et al.* 2000; Fricke *et al.* 2001). These observations led to a model in which Sgs1 creates a DNA substrate that requires Top3 activity for its resolution.

In vitro, *E. coli* RecQ and Topo III demonstrate a concerted DNA strand passage activity that neither enzyme can perform alone. Together, RecQ and Topo III catenate/decatenate or remove positive supercoils from covalently closed dsDNA molecules (Harmon *et al.* 1999, 2003). Evidence supports a model in which Topo III recognizes the DNA structure at the unwound DNA fork bound to RecQ and is stimulated to perform sequential ssDNA passage events on opposing DNA strands, thus effectively achieving a dsDNA strand passage event. A similar concerted enzymatic activity is seen cross-species with bacterial RecQ and budding yeast Top3 as well as with mammalian Blm–Topo III, indicating that this functional interaction is conserved (Harmon *et al.* 1999; Wu and Hickson 2002, 2003). Furthermore, the conservation of a protein–protein interaction domain in eukaryotic RecQ homologs that specifically interacts with Topo III speaks to the biological importance of a concerted RecQ–Topo III activity.

The *in vivo* substrate for RecQ–Topo III is not known. Since the *top3* mutant phenotype is largely suppressed by *sgs1* in yeast, the severe defects caused by loss of Top3 are likely due to incomplete processing of intermediates that arise when Sgs1 acts alone. In bacteria and yeast, Topo III mutant defects are also suppressed when homologous recombination is eliminated (Gangloff *et al.* 1999; Zhu *et al.* 2001; Oakley *et al.* 2002; Shor *et al.* 2002; Laursen *et al.* 2003). Furthermore, *top3* mutant sensitivities to agents that cause DNA lesions or replication fork stall are suppressed by *sgs1* (Chakraverty *et al.* 2001) and it has been suggested that Sgs1 functions in the stabilization of stalled replication forks (Cobb *et al.* 2003). These observations contributed to the proposal that RecQ–Topo III is important for the resolution of recombination intermediates that form during DNA replication. Further support for this notion comes from recent studies of the Holliday junction dissolution seen *in vitro* with the Blm–TopoIII complex (Wu *et al.* 2005).

To further our understanding of RecQ–Topo III biology, we searched for gene dosage suppressors of *top3* in *S. cerevisiae* and identified a single gene, *PIF1*, which encodes a DNA helicase that acts with polarity that is opposite to that of Sgs1. Although Pif1 overexpression suppresses multiple *top3* defects, it exacerbates *sgs1* and *sgs1 top3* defects. We find that Pif1 helicase activity is essential in *top3* mutants and that this requirement is dependent upon both an active Sgs1 DNA helicase and homologous recombination. Homologous recombination proteins form nuclear DNA repair foci spontaneously during S phase and in response to DNA damage (Lisby *et al.* 2001; Lisby *et al.* 2003) and here we show that Pif1 localizes to these same DNA repair foci. The frequency of Pif1 foci is significantly increased in *top3* mutant cells, suggesting that Pif1 is recruited to sites of DNA damage when Sgs1 acts without Top3. Our results demonstrate that the Pif1 DNA helicase is required to prevent or repair recombination-dependent DNA damage that arises when Sgs1 helicase activity is uncoupled from Top3.

MATERIALS AND METHODS

Media: Yeast extract–peptone–dextrose (YPD), synthetic complete (SC), and 5-flouroorotic acid (5-FOA) media were made as described (Sherman *et al.* 1986) with twice the recommended amount of leucine. Sporulation medium was prepared as described (Klapholz and Esposito 1982).

Strains, plasmids, and genetic manipulations: The yeast strains used in this study are listed in Table 1. Mating, sporulation, and dissections were performed by standard procedures (Sherman *et al.* 1986). For segregation analysis of synthetic gene interactions, a minimum of 80 tetrads were dissected in each case. Unless otherwise indicated, cells were maintained at 30°. Temperature-sensitive strains were grown at 23° and 37° for permissive and restrictive conditions, respectively. For microscopic examination of fluorescently tagged proteins, cells were grown at 23° to allow for optimal formation of the fluorophore. Transformation of DNA into yeast was performed by standard methods (Gietz and Woods 2002). Genetic manipulations involving polymerase chain reaction (PCR)-generated DNA fragments were confirmed by DNA sequence analysis. Relevant plasmid details are summarized in Table 2. Oligonucleotide sequences are given in supplemental Table 1 at http://www.genetics.org/supplemental/.

Plasmid pWJ659 (gift from J. Weinstein) was made by subcloning a blunt-ended 2.6-kb *Xba*I–*Fsp*I *TOP3* fragment from pWJ171 (Wallis *et al.* 1989) into the *Sma*I site of pRS415

TABLE 1

Strains used in this study

Strain	Genotype
W1588-4C	*MAT***a** *ade2-1 can1-100 his3-11,15 leu2-3,112 trp1-1 ura3-1*
J1022[a]	*MAT***a** *top3–E447K, S583L*
W3966-18A[a]	*MAT*α *top3–E447K, S583L iYLR237::TRP1*
W3040[a]	*MAT***a**/*MAT*α *top3–Y356F/TOP3*
W3040-9A[a]	*MAT***a** *top3–Y356F* pWJ1189
W1958[b]	*MAT***a**/*MAT*α *top3::TRP1/TOP3 sgs1::HIS3/SGS1*
W3609-5D[a]	*MAT***a** *pif1::URA3*$^{K.l.}$
J1129[a]	*MAT***a** *pif1*Δ
W3642[a]	*MAT***a**/*MAT*α *top3::TRP1/TOP3 sgs1::HIS3/SGS1 pif1::URA3*$^{K.l.}$*/PIF1*
W5290-3B[a]	*MAT*α *pif1::KAN-MX*
W4168-2B[a]	*MAT***a** *pif1-K264R*
W3972-7C[a]	*MAT***a** *pif1-m2*
W3732-1C[a]	*MAT***a** *rrm3::URA3*$^{K.l.}$
J1132[a]	*MAT***a** *rrm3*Δ
W3656[a]	*MAT***a**/*MAT*α *rrm3::URA3*$^{K.l.}$*/RRM3 top3::TRP1/TOP3 sgs1::HIS3/SGS1*
W2069-2B[b]	*MAT***a** *sgs1-*Δ*N82*
W1911-1B[b]	*MAT***a** *sgs1–K706R*
W2075-3C[b]	*MAT***a** *sgs1-*Δ*N82, K706R*
W5488	*MAT***a**/*MAT*α *pif1::KAN-MX/PIF1 sgs1::HIS3/SGS1-LEU2*
W5493	*MAT***a**/*MAT*α *pif1::KAN-MX/PIF1 sgs1-*Δ*N82/SGS1-LEU2*
W5491	*MAT***a**/*MAT*α *pif1::KAN-MX/PIF1 sgs1–K706R/SGS1-LEU2*
W5495	*MAT***a**/*MAT*α *pif1::KAN-MX/PIF1 sgs1-*Δ*N82, K706R/SGS1-LEU2*
W5497	*MAT***a**/*MAT*α *pif1::KAN-MX/PIF1 sgs1–K706R/SGS1-LEU2 top3::TRP1/TOP3* . . .
J911[c]	*MAT***a** *rad51*Δ
W2263-1B[d]	*MAT*α *rad52::HIS5*
W3248-1A[e]	*MAT*α *rad54::LEU2*
W3572-6C[e]	*MAT*α *rad55*Δ
W3868	*MAT***a**/*MAT*α *top3::TRP1/TOP3 pif1::URA3*$^{K.l.}$*/PIF1 rad54::LEU2/RAD54*
W3869	*MAT***a**/*MAT*α *top3::TRP1/TOP3 pif1::URA3*$^{K.l.}$*/PIF1 rad55*Δ*/RAD55* . . .
W1518-3C[f]	*MAT*α *rad9::HIS3 top3::LEU2*
W2972-1C[g]	*MAT***a** *mad2-1*
W3831-1B[a]	*MAT***a** *CUP1::URA3-SUP11-***o**
W3480-4C[a]	*MAT***a** *rDNA::URA3*
W1868-8B[a]	*MAT***a** *SUP4-***o***::URA3*
W2297-1A[h]	*MAT***a** *RAD52–YFP ADE2 bar1::LEU2*
W4436[a]	*MAT***a**/*MAT*α *top3::TRP1/TOP3 RAD52–YFP/RAD52–YFP ADE2/ADE2 lys2/LYS2 bar1::LEU2/BAR1*
W2312-16A[i]	*MAT***a** *RAD52–CFP ADE2 bar1::LEU2*
W4180-8D[a]	*MAT***a** *PIF1–YFP ADE2 bar1::LEU2*
W4240-25B[a]	*MAT***a** *PIF1–YFP RAD52–CFP bar1::LEU2*
W4294-8D[a]	*MAT***a** *RRM3–YFP ADE2 bar1::LEU2*
W3653[a]	*MAT***a**/*MAT*α *top3::TRP1/TOP3 sgs1::HIS3/SGS1 RAD52–YFP/RAD52 trp1-1/TRP1 lys2*Δ*/LYS2 ADE2/ADE2 bar1::LEU2/bar1::LEU2*
W4238[a]	*MAT***a**/*MAT*α *top3::TRP1/TOP3 RAD52–CFP/RAD52 PIF1–YFP/PIF1 ADE2/ADE2 bar1::LEU2/bar1::LEU2*
W2926[a]	*MAT***a**/*MAT*α *top3::TRP1/TOP3 sgs1::HIS3/SGS1 RAD52–YFP/RAD52–YFP trp1-1/TRP1 lys2*Δ*/LYS2 ADE2/ADE2 bar1::LEU2/bar1::LEU2*
W4197[a]	*MAT***a**/*MAT*α *top3::TRP1/TOP3 PIF1–YFP/PIF1 ADE2/ADE2 bar1::LEU2/bar1::LEU2*
W4294[a]	*MAT***a**/*MAT*α *RRM3–YFP/RRM3 top3::TRP1/TOP3 ADE2/ADE2 bar1::LEU2/BAR1*

All strains are derived from W303 (Thomas and Rothstein 1989). Unless otherwise indicated, all strains are isogenic to W1588-4C (Zou and Rothstein 1997). *URA3*$^{K.l.}$ refers to *URA3* from *Kluyveromyces lactis*, an ortholog of *S. cerevisiae URA3*. In cases in which multiple strains of identical genotype were used, one example is given. All strains are from the Rothstein Lab.

[a] From this study.
[b] Gift of J. Weinstein.
[c] Gift of Q. Feng.
[d] Gift of A. Antúnez de Mayolo.
[e] From Shor *et al.* (2002).
[f] Gift of X. Zhao.
[g] Gift of R. Reid.
[h] From Lisby *et al.* (2001).
[i] From Lisby *et al.* (2003).

TABLE 2

Plasmids used in this study

Plasmid	Relevant genotype[a]	Source
pWJ659	*CEN LEU2 TOP3*	Gift of J. Weinstein
pWJ171	*CEN LEU2 TOP3*	Wallis *et al.* (1989)
pRS415	*CEN LEU2*	Sikorski and Hieter (1989)
pWJ1092	*CEN URA3 TOP3*	This study
pWJ1114	*URA3 TOP3*	This study
YCp50	*CEN URA3 TOP3*	Rose *et al.* (1987)
pRS306	*URA3*	Sikorski and Hieter (1989)
pWJ1130	*CEN URA3 top3–E447K, S583L*	This study
pWJ1203	*URA3 top3–E447K, S583L*	This study
pRS304	*TRP1*	Sikorski and Hieter (1989)
pWJ1174	*TRP1 iYLR237*	This study
pRS425	2μ *LEU2*	Sikorski and Hieter (1989)
pRS1372	2μ *LEU2 top3–E447K, S583L*	This study
pWJ1047	*CEN URA3 Gal*-A-*Hpa*I-B	Gift of R. Reid
pWJ1067	*CEN URA3 Gal-TOP3*	This study
pWJ1074	*CEN URA3 Gal-top3–Y356F*	This study
pWJ1085	*CEN LEU2 top3–Y356F*	This study
pWJ1113	*URA3 top3–Y356F*	This study
pRS417	*CEN ADE2*	Brachmann *et al.* (1998)
pWJ1189	*CEN URA3 ADE2 TOP3*	This study
pWJ1279	*CEN URA3 Gal-PIF1*	This study
pWJ1280	*CEN URA3 Gal-pif1–K264R*	This study
pWJ1281	*CEN URA3 Gal-RRM3*	This study
pWJ1345	*CEN HIS3 Gal*-A-*Hpa*I-B	This study
pWJ1346	*CEN HIS3 Gal-TOP3*	This study
pWJ1347	*CEN HIS3 Gal-top3–Y356F*	This study
pUH7	*ura3::HIS3*	Cross (1997)
pRS413	*CEN HIS3*	Sikorski and Hieter (1989)
pWJ1315	*CEN HIS3 NUP49*	This study
pWJ1323	*CEN HIS3 CFP-NUP49*	This study
pRS416	*CEN URA3*	Sikorski and Hieter (1989)
pWJ1348	*CEN URA3 CFP-NUP49*	This study
pLH7	*leu2::HIS3*	Cross (1997)
pCox4-DsRed.T4	*CEN LEU2 COX4–DsRed*	Bevis and Glick (2002)
pWJ1326	*CEN HIS3 COX4–DsRed*	This study
pWJ1249	*CEN TRP1* C-*Hpa*I-D	Gift of R. Reid
pWJ1277	*CEN HIS3 NOP1*	This study
pWJ1299	*CEN HIS3 NOP1–CFP*	This study
pWJ1327	*CEN URA3 NOP1–CFP*	This study
pWJ1321	*CEN HIS3 NOP1–DsRed*	This study
pWJ1322	*CEN URA3 NOP1–DsRed*	This study
YEp51B	2μ *LEU2*	Akada *et al.* (1997)
Clone 1	2μ *LEU2 PIF1*	Akada *et al.* (1997)
Clone 2	2μ *LEU2 PIF1*	Akada *et al.* (1997)
HCS2	2μ *LEU2 TOP3*	Akada *et al.* (1997)
pWJ1246	Clone 1 + Δ*pif1*	This study
pWJ1286	Clone 1 + *pif1–K264R*	This study
pL1580	*CUP1::URA3-SUP11-***o**	Keil and McWilliams (1993)

[a] Plasmid sequences and/or maps are available upon request.

(Sikorski and Hieter 1989). Respectively, plasmids pWJ1092 and pWJ1114 were made by subcloning *TOP3* from pWJ659 into YCp50 (Rose *et al.* 1987) and pRS306 (Sikorski and Hieter 1989) via *Bam*HI and *Hin*dIII sites. To make plasmid pWJ1189 (*CEN–URA3–ADE2–TOP3*), the *Bgl*II *ADE2* fragment from pRS417 (Brachmann *et al.* 1998) was subcloned into the *Bam*HI site of pWJ1092.

The *top3–E447K,S583L* conditional allele (*top3-ts*) was isolated from a genetic screen. Briefly, a randomly mutagenized pool of *TOP3* open reading frames (ORFs) was generated by PCR (primers TOP3 + 124-R and TOP3 − 84-F) and cotransformed with *Sna*BI- and *Pvu*II-gapped pWJ1092 into a *top3::TRP1* haploid, thus allowing recombination-mediated formation of a *top3* mutant plasmid library *in vivo*. Transformants were assayed for growth and MMS sensitivity at 23°

and 37° and plasmids containing *top3-ts* candidates rescued for further analysis. *Bona fide top3-ts* candidates were integrated at the endogenous locus via standard allele replacement methods (described in Rothstein 1991). The integration plasmid pWJ1203 was made by subcloning the E447K, S583L missense mutations from the original library isolate pWJ1130 into pWJ1114 via *Bss*HII and *Bst*WI sites. The *top3–E447K, S583L* strain has the desired *ts* phenotype and both missense mutations are required for this phenotype. To mark the *TOP3* locus with *TRP1*, a 931-bp fragment from intergenic region iYLR237 was amplified by PCR (primers F-*Xba*I-iYLR237 and R-*Cla*I-iYLR237), digested with *Xba*I and *Cla*I and subcloned into pRS304 (Sikorski and Hieter 1989) to make pWJ1174, which was then linearized and integrated at the endogenous iYLR237 locus. To show hypomorphism, *top3–E447K,S583L* was subcloned from pWJ1203 into pRS425 (Christianson *et al.* 1992) via *Bam*HI and *Sal*I sites to make the *top3-ts* high-copy vector pWJ1372.

The *top3–Y356F* catalytically inactive allele was first constructed in plasmid pWJ1074 (see below) and the Y356F mutation subcloned into pWJ659 via *Sph*I and *Blp*I sites to make plasmid pWJ1085. Using *Bam*HI and *Hin*dIII sites the *top3–Y356F* allele was subcloned from pWJ1085 into pRS306 (Sikorski and Hieter 1989) to generate vector pWJ1113 that was then integrated at the endogenous *TOP3* locus yielding a *TOP3–URA3–top3–Y356F* repeat (strain U515). Recombinant pop-outs selected on 5-FOA only gave *TOP3* isolates, suggesting that *top3–Y356F* is lethal. Plasmid pWJ659 transformed into U1515 provides wild-type *TOP3* in *trans* and allowed successful recovery of *top3–Y356F* integrants. The *top3–Y356F* + pWJ659 strain was crossed to a wild-type strain. Loss of pWJ659 from the heterozygous diploid followed by sporulation and segregation analysis demonstrated that a *top3–Y356F* strain is inviable. *top3–Y356F* spore products germinate and form microcolonies (2–100 cells) that do not grow upon restreak. Plasmid shuffle to replace pWJ659 with pWJ1189 yielded the haploid *top3–Y356F* strain covered by plasmid-borne *TOP3* that was used in the gene dosage suppressor screen (W3040-9A). Consistent with *top3–Y356F* lethality, strain W3040-9A cannot lose pWJ1189, as evidenced by lack of growth on 5-FOA.

The *pif1::URA3*$^{K.l.}$ and *rrm3::URA3*$^{K.l.}$ strains were made by described methods (Reid *et al.* 2002a,b) using the appropriate intergenic primers (Research Genetics) and *URA3*$^{K.l.}$ pop-outs selected on 5-FOA. The *pif1::KAN-MX* deletion allele was amplified with intergenic primers (Research Genetics) from the appropriate deletion consortium library strain (Winzeler *et al.* 1999) and transferred to W1588-4C as described (Reid *et al.* 2002a,b).

The catalytically inactive *pif1–K264R* allele was amplified from plasmid pWJ1280 (see below) and integrated at the endogenous locus via allele replacement methods (Erdeniz *et al.* 1997) using primers C-PIF1-484F and D-PIF1-919R. The *pif1-m2* allele was made by oligonucleotide-directed mutagenesis/PCR fusion using primers C-PIF1-us45-F, delATG2-Rev, delATG2-For, and Pif1-302R-D and integrated by similar methods. The *sgs1-K706R*, *sgs1-ΔN82*, and *sgs1-ΔN82, K706R* strains were gifts from J. Weinstein.

Plasmids containing galactose-inducible genes were made as follows. Plasmid pWJ1047 contains a galactose-inducible promoter followed by an *Hpa*I restriction site that is flanked by A- and B-adaptamer sequence (gift from R. Reid). Respectively, A- and B-adaptamers correspond to the sequences appended to the N- and C-terminal ORF primers available from Research Genetics (Hudson *et al.* 1997). The appropriate ORF primers were used to amplify *TOP3*, *PIF1*, and *RRM3*, and the resulting PCR products cotransformed into yeast with *Hpa*I-linearized pWJ1047 to make vectors pWJ1067, pWJ1279, and pWJ1281, respectively, by *in vivo* recombination. The *top3–Y356F* allele was made via oligonucleotide-directed mutagenesis/PCR fusion (primers TOP3-YF-fwd, TOP3-YF-rev, and Research Genetics ORF primers for *TOP3*) and subcloned into plasmid pWJ1047 to make plasmid pWJ1074 via adaptamer-mediated *in vivo* recombination. The *pif1–K264R* missense mutation was made by oligonucleotide-directed mutagenesis/PCR fusion with primers PIF1-333-F, PIF1-K264R-R, PIF1-K264R-F, and PIF1-1467-R, and the resulting DNA fragment digested with *Pme*I and *Sac*II and subcloned into pWJ1279 to make pWJ1280. Replacement of *URA3* with *HIS3* using the marker-swap cassette from pUH (Cross 1997) converted plasmids pWJ1047, pWJ1067, and pWJ1074 to plasmids pWJ1345, pWJ1346, and pWJ1347, respectively.

A C-terminal fusion of *YFP* to *PIF1* was made at the endogenous locus via described methods (Reid *et al.* 2002a) using primers C-Pif1-g-up, C-Pif1-gfuse-up, C-Pif1-g-down, and C-Pif1-gfuse-down. Similarly, a C-terminal fusion of *YFP* to *RRM3* was made at the endogenous locus using primers C-Rrm3-g-up, C- Rrm3-gfuse-up, C- Rrm3-g-down, and C- Rrm3-gfuse-down. Plasmid pWJ1326 was made by replacing the *LEU2* marker of plasmid pCox4–DsRed.T4 (Bevis and Glick 2002) with *HIS3* using the marker-swap cassette from pLH (Cross 1997).

For construction of *CFP–NUP49*, first a plasmid expressing Nup49 from its endogenous promoter was constructed by amplifying genomic *NUP49* (primers Nup49fwd and Nup49bwd), digesting the DNA fragment with *Sca*I and *Msl*I followed by subcloning into the *Sma*I site of pRS415 (Sikorski and Hieter 1989) and subsequent subcloning into pRS413 (Sikorski and Hieter 1989) via *Sac*I and *Xho*I sites to make plasmid pWJ1315. Next, *CFP* coding sequence was fused to the 5′-end of endogenous *NUP49* as described (Reid *et al.* 2002a) using primers Nup49fwd, Nup49-Tup, Nup49-Tdown, and Nup49down. Integration/pop-out of the *URA3*$^{K.l.}$ marker was performed under cover of pWJ1315 since the *CFP–URA3*$^{K.l.}$*–CFP–NUP49* fusion is a null allele of an essential gene. The resulting *CFP–NUP49* fusion was incorporated into plasmid pWJ1315 via gap repair to make plasmid pWJ1323. Plasmid pWJ1348 was made by subcloning *CFP–NUP49* from pWJ1323 into pRS416 (Sikorski and Hieter 1989) via *Bam*HI and *Sal*I sites.

Construction of the *NOP1* plasmids was as follows. Plasmid pWJ1249 contains an *Hpa*I restriction site flanked by C- and D-adaptamer sequence (gift from R. Reid). C- and D-adaptamers correspond to the sequences appended to the intergenic primers available from Research Genetics. First, a plasmid expressing Nop1 from its endogenous promoter was made via adaptamer-mediated *in vivo* recombination by cotransforming *NOP1* that had been amplified from genomic DNA using the appropriate intergenic primers (Research Genetics) and *Hpa*I-linearized pWJ1249. *NOP1* was subsequently subcloned from pWJ1249 into pRS413 via *Sac*I and *Xho*I sites to make plasmid pWJ1277. Next, *CFP* coding sequence was integrated at the 3′-end of endogenous *NOP1* as described (Reid *et al.* 2002a) using primers Nop1-g-up, Nop1-gfuse-up, Nop1-gfuse-down, and Nop1-g-down. Integration was performed in a diploid since the *NOP1–CFP–URA3*$^{K.l.}$*–CFP* haploid is inviable. *NOP1–CFP* was then amplified from the integrated repeat in two overlapping parts (primers Nop1-g-up, XFP-3′int, XFP-5′int, and Nop1-g-down) and the PCR products cotransformed with *Cla*I and *Sex*AI gapped pWJ1277 to generate the *NOP–CFP* plasmid pWJ1299 by a three-part *in vivo* recombination. Plasmid pWJ1327 was made by subcloning *NOP1–CFP* from pWJ1299 to pRS416 (Sikorski and Hieter 1989) via *Xho*I and *Not*I sites. Plasmid pWJ1321 was made by gap-repair/exchange of *CFP* (pWJ1299) with *DsRed*. pWJ1322 was made by subcloning *DsRed–NOP1* from pWJ1321 into pRS416 (Sikorski and Hieter 1989) via *Sac*I and *Xho*I sites.

Genetic screens: *Screen for high-copy suppressors of top3Δ slow growth:* A homozygous *top3Δ* diploid was used for two reasons: (1) the likelihood of recovering recessive loss of function mutations that suppress *top3* (*e.g.*, *sgs1*) as false positives is reduced and (2) the greater severity of the *top3* phenotype in diploids *vs.* haploids is more amenable to suppressor analysis. The *top3Δ* diploid is so sickly that it must be maintained by providing a plasmid-borne copy of wild-type *TOP3* and a plasmid shuffle strategy was used for the screen. A homozygous *top3::TRP1* null diploid harboring plasmid pWJ1189 (*CEN–URA3–ADE2–TOP3*) was transformed with a high-copy yeast genomic library contained in vector YEp51B (2μ-*LEU2*) (Akada *et al.* 1997). Normally, the *top3* diploid cannot lose pWJ1189 as evidenced by sensitivity to 5-FOA, a compound that counterselects *URA3*. Library transformants were selected on SC-Leu in the presence of uracil to permit random loss of pWJ1189 in isolates containing suppressors of *top3* and subsequently replica plated to 5-FOA-Leu. Transformants that gave rise to 5-FOA^r colonies were assayed for ability to grow on SC-Ade to confirm loss of pWJ1189. 5-FOA^r, Ade− transformants were chosen as candidate suppressors for further analysis. The HCS2 clone isolated in this screen contains *TOP3* and serves as a control plasmid in several experiments. A single plasmid-linked, non-*TOP3* high-copy suppressor, designated clone 1 (Figure 1A), was obtained. Clone 1 also suppresses *top3Δ* slow growth in a haploid. Plasmid pWJ1246 deletes the 1277-bp *Sac*II fragment from clone 1 encompassing the C-terminal half of *PIF1* and does not suppress *top3* defects. Plasmid pWJ1286 was made by subcloning the *pif1–K264R* mutation from pWJ1280 into clone I via *Bsu*361 and *Pme*I sites. We found that pWJ1286 suppresses *top3* defects as well as clone 1 in *top3 PIF1* strains.

To test whether pWJ1286 can suppress in the complete absence of wild-type Pif1 (*top3Δ pif1Δ* strains), we employed a plasmid shuffle strategy analogous to the original screening process. First, a *top3Δ pif1Δ* strain harboring pWJ1189 (*TOP3*) was generated by transformation of a *top3Δ pif1Δ* heterozygote with pWJ1189 followed by sporulation and selection of the desired haploid segregant. Next, the *top3Δ pif1Δ* pWJ1189 haploid was transformed with YEp51B, clone 1, or pWJ1286. The resulting transformants were tested for their ability to lose pWJ1189 by growing first on SC-Leu and then replica plating to 5-FOA-Leu. Only clone 1 allowed loss of pWJ1189; growth on 5-FOA for pWJ1286-containing isolates was nonexistent and indistinguishable from YEp51B-containing isolates.

Screen for high-copy suppressors of top3-ts slow growth: This screen was performed in a *top3-ts* (*top3–E447K,S583L*) homozygous diploid using the same 2μ genomic library described above. Since the *top3-ts* diploid grows as well as a wild-type strain at 23°, there is no need to provide a plasmid-borne copy of wild-type *TOP3*, thus simplifying the screening method. A *top3-ts* homozygote was transformed with the YEp51B genomic library and transformants selected on SC-Leu at 23°. Colonies were subsequently replica plated to a fresh SC-Leu plate and incubated at 37°. Transformants exhibiting robust growth at the restrictive temperature were chosen as candidates. One plasmid-linked, non-*TOP3* high-copy suppressor was identified and is designated clone 2 (Figure 1A).

Screen for high-copy suppressors of top3–Y356F lethality: A *top3–Y356F* haploid is viable only when wild-type *TOP3* is provided in *trans*. A *top3–Y356F* haploid harboring pWJ1189 was transformed with the YEp51B high-copy library and suppressors sought via a plasmid shuffle strategy as described above for the *top3Δ* high-copy suppressor screen. Recessive chromosomal loss-of-function mutations were frequently isolated as false-positive candidates and were eliminated by standard complementation testing. All candidates eliminated by this criterion were determined to be *sgs1* mutations. No plasmid-linked, non-*TOP3* high-copy suppressors were identified in this screen.

Microscopy: Cells were processed for fluorescent microscopy and mounted on slides as described previously (Lisby *et al.* 2001). Live cell images were captured with a cooled Orca-ER CCD camera (Hamamatsu, Japan) mounted on a Zeiss Axioplan 2 microscope (Carl Zeiss, Thornwood, NY) using a Plan-Apochromat 100×, 1.4 NA objective lens and 100 W mercury arc lamp (Osram, Munich, Germany). For each field of cells, 11 or 13 fluorescent images at each of the relevant wavelengths were obtained at 0.3-μm intervals along the *z*-axis to allow inspection of all focal planes of each cell. Images were acquired and pseudo-colored using OpenLab software (Improvision, Lexington, MA) and prepared for publication in Adobe Photoshop (Adobe, San Jose, CA). The fluorophores used in this study and the filters used to visualize them are as described (Lisby *et al.* 2003).

Recombination assays: The recombination frequency between the δ-repeats at the *SUP4* locus was determined as described (Rothstein *et al.* 1987; Wallis *et al.* 1989). W1588 (W303) strains have ochre-suppressible mutations at *ADE2* and *CAN1*. The *URA3* selectable marker is inserted between δ-repeats 4 and 5 at the *SUP4* locus, thus linking it to the *SUP4-o* dominant allele. To measure the recombination frequency between δ-repeats, simultaneous loss of *URA3* and *SUP4-o* was assessed by monitoring adenine prototrophy and both canavanine and 5-FOA resistance. For determination of the recombination frequency between rDNA repeats at the rDNA locus, an *RDN::URA3* assay (Zou and Rothstein 1997) was crossed into the appropriate genetic backgrounds, single segregants were picked from an SC-Ura plate, grown overnight in liquid SC-Ura, and then plated to 5-FOA medium to determine the frequency of *URA3* loss. The total number of colony-forming units (cfu) analyzed was determined by direct plating to SC and the deletion frequency calculated accordingly. A recombination assay was placed at the *CUP1* locus via integration of *Xba*I-linearized plasmid pL1580 (gift of R. Keil) and crossed into the appropriate mutant backgrounds. Similar to the method used to measure recombination at rDNA, the recombination frequency between *CUP1* repeats was determined by measuring 5-FOA resistance as described (Keil and McWilliams 1993). All recombination assays were performed in the relevant null mutant backgrounds with the exception of the *SUP4-o* assay in which the *pif1-m2* allele was used because the petite phenotype of *pif1Δ* interferes with the red/white color assay that is used to assess adenine prototrophy.

Miscellaneous methods: For determination of the doubling time of yeast strains, cultures were maintained in mid-log phase in SC-Leu and cell density was monitored over time with a spectrophotometer. Analysis of cell-cycle distribution was performed on log-phase cultures by microscopic examination. Cells were scored as G1 (unbudded), S (small budded), or G2/M (large budded). Classification as S *vs.* G2/M was based on both position of the nucleus as determined by a nuclear marker (Rad52 or Nup49) or DAPI staining and bud size. Cells with a bud less than or equal to one-third the size of the mother and a nucleus still in the mother cell were classified as S phase. Cells with a bud greater than one-third the size of the mother with the nucleus at or in the neck were classified as G2/M. Nuclear position was used as the overriding criterion. To determine the effect of p2μ-*PIF1* on cell-cycle distribution, over 750 cells were viewed for each culture. To determine plating efficiency, quadruplicate cultures of cells were grown to mid-log phase in SC-Leu, quantitated in a hemacytometer, 200 cells plated per SC-Leu plate, and the plates incubated for 3 to 4 days. Plating efficiency was calculated as the number of cfu divided by the number of cells plated. In this same experiment, the frequency of spontaneous petite formation

(mitochondrial deficiency) was determined by replica plating from SC-Leu to media containing glycerol (a nonfermentable sugar) as the sole carbon source. Since petites cannot grow on nonfermentable carbon sources, the frequency of petite formation could be determined as the number of cfu that do not grow on glycerol divided by the total cfu. To examine the effect of co-overexpressing *TOP3* and *PIF1* alleles in a wild-type strain background, a galactose-inducible series of vectors was used. The *TOP3* series (pWJ1345, pWJ1346, and pWJ1347) was transformed into a wild-type *MAT***a** strain, and the *PIF1* series (pWJ1047, pWJ1279, and pWJ1280) was transformed into a wild-type *MAT*α strain. The two sets of resulting transformants were then mated to each other and diploids were selected on SC-Ura,His and streaked onto SGal-Ura,His medium. Similarly, pGal-*RRM3* (pWJ1281) was transformed into the wild-type MATα strain and diploids were made to test the effect of co-overexpressing *RRM3* and the *TOP3* plasmid series.

Gamma irradiation was administered using a Gammacell-220 ^{60}Co irradiator (Atomic Energy, Ottawa, Canada). To determine gamma-ray sensitivities of strains, cells were grown to mid-log phase and then plated on YPD. YPD plates were exposed to varying doses (0–80 krad) of gamma. For analysis of Rad52 and Pif1 focus formation in response to gamma rays, cultures were grown to mid-log phase and exposed to 4 krad of gamma rays and aliquots of cells were taken and subjected to fluorescence microscopy for a 3-hr time course. Two trials yielded similar results and the data were compiled with over 2100 cells viewed postirradiation.

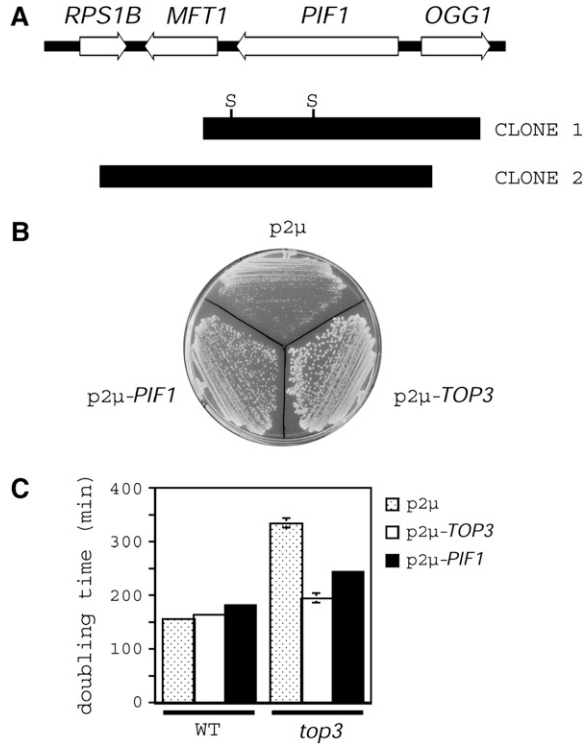

FIGURE 1.—Pif1 is a multicopy suppressor of *top3* mutant defects. (A) Overlapping nonidentical clones of *PIF1* were identified in screens for high-copy suppressors of *top3* slow growth. Clones 1 and 2 encompass 148,448–152,810 bp and 146,813–152,060 bp from chromosome XIII, respectively. Removal of the 1277-bp *Sac*II (S) fragment from clone 1 that encompasses the C-terminal half of Pif1 eliminates suppression. (B) High-copy Pif1 suppresses *top3* slow growth. The plate shows colony streaks of a *top3*Δ haploid transformed with the indicated vectors. (C) The graph indicates the doubling times at 30° for wild-type and *top3*Δ strains harboring the indicated vectors. Strains: wild type (W1588-4C), *top3*Δ (W1958 haploid segregant). Plasmids: p2μ (YEp51B), p2μ-*TOP3* (HCS2), p2μ-*PIF1* (clone 1).

RESULTS

A search for high-copy suppressors in three different *top3* mutant backgrounds: A *top3*Δ strain exhibits multiple defects including slow growth, sensitivity to DNA damaging agents, a cell-cycle defect characterized by an accumulation of cells in G2/M, reduced cell viability, and hyperrecombination at repetitive sequences. Three *top3* allelic backgrounds were used to search for high-copy suppressors. The first is a *top3* null allele (*top3*Δ). The next is a hypomorphic *top3-ts* conditional allele that we isolated, which behaves like wild type at the permissive temperature and *top3*Δ at the restrictive temperature. The third is a catalytically inactive *top3–Y356F* allele, which contains phenylalanine substituted for the active site tyrosine that covalently binds to the free DNA end during the Top3 catalytic cycle (BENNETT and WANG 2001). We found that this *top3–Y356F* strain is inviable. Gene dosage suppressors of *top3* mutant slow growth—or in the case of *top3–Y356F*, lethality—were isolated as described in MATERIALS AND METHODS. In the *top3*Δ background, 60,000 transformants yielded 27 plasmid-linked suppressors, 26 of which contained *TOP3*. One plasmid, designated clone 1, contains a genomic fragment from chromosome 13 (Figure 1A). Figure 1B shows suppression of *top3*Δ slow growth by clone 1. In the *top3-ts* background, 600,000 transformants yielded 218 plasmid-linked suppressor clones, 217 of which contained *TOP3*. One isolate, designated clone 2, contains a genomic fragment from chromosome 13 that is distinct from, but overlaps, clone 1 (Figure 1A). In the *top3–Y356F* background, 500,000 transformants yielded 203 plasmid-linked suppressors, all of which contained genomic clones of *TOP3*.

PIF1 encodes a 5′-to-3′ DNA helicase that functions in both nuclear and mitochondrial DNA metabolism (reviewed in BESSLER *et al.* 2001) and is the only complete open reading frame common to clones 1 and 2. Deletion of the C-terminal half of *PIF1* removes conserved helicase domains that are essential to catalytic activity and eliminates the ability of clone 1 to suppress *top3* slow growth, confirming that *PIF1* is the high-copy suppressor (Figure 1A and data not shown). The *PIF1* gene has two distinct start codons (SCHULZ and ZAKIAN 1994). Protein translated from the first ATG includes a mitochondrial targeting signal sequence, and protein translated from the second ATG lacks this sequence and is destined for the nucleus. Absence of mitochondrial Pif1 leads to mitochondrial DNA loss and a mitochondrial-deficient or petite yeast strain. Nuclear roles ascribed to Pif1 include maintenance of telomeric and ribosomal DNA.

TABLE 3

High-copy *PIF1* suppresses the *top3*Δ cell-cycle defect

		% of cells in each cell-cycle stage[a]		
		G1	S	G2/M
Wild type	+ p2μ	54	23	23
	+ p2μ-*PIF1*	52	24	24
	+ p2μ-*pif1-KR*	53	23	24
*top3*Δ	+ p2μ	34	17	49
	+ p2μ-*PIF1*	50	20	30
	+ p2μ-*pif1-KR*	50	21	29

[a] As described in MATERIALS AND METHODS, cell-cycle stage classification was determined via microscopy on the basis of both cellular morphology and nuclear position. Over 750 cells from logarithmic cultures grown in SC-Leu were viewed for each strain + plasmid background. Strains used are W1588-4C (*MAT***a** *TOP3*) and a W1958 haploid segregant (*MAT***a** *top3::TRP1*). Plasmids used are the *LEU2*-marked YEp51B (p2μ), clone 1 (p2μ-*PIF1*), and pWJ1286 (p2μ-*pif1-KR*).

***PIF1* is a gene dosage suppressor of multiple *top3* mutant defects:** Consistent with the finding that high-copy *PIF1* suppresses *top3*Δ slow growth as evidenced on plate assays (Figure 1B), high-copy *PIF1* shortens *top3*Δ doubling time in liquid culture (Figure 1C). The generation time of the *top3*Δ strain is 334 min and this is reduced to 194 min by p2μ-*TOP3*. High-copy *PIF1* shortened the doubling time of the *top3*Δ strain to 244 min, demonstrating partial suppression of *top3*Δ slow growth. In contrast, the generation time of the wild-type strain (156 min) is slightly lengthened by p2μ-*PIF1* (181 min) in our strain background (W303; W1588). This is consistent with previous reports that Pif1 overexpression causes slow growth in wild-type cells (LAHAYE *et al.* 1991). In addition, we found that high-copy Pif1 (p2μ-*PIF1*) reduced the plating efficiency of wild-type cells (W1588-4C) from 100 ± 0.5% to 51 ± 2%. On the other hand, Pif1 overexpression did not reduce plating efficiency (39 ± 4%) in *top3*Δ cells (W1958 segregants), which normally have a plating efficiency of 33 ± 4%.

The effect of high-copy *PIF1* on the cell cycle was examined by microscopy as described in MATERIALS AND METHODS (Table 3). The cell-cycle profile of a log-phase wild-type culture is unaltered by p2μ-*PIF1*. Mutant *top3*Δ cells accumulate in G2/M and p2μ-*PIF1* partially rescues this defect. These data suggest that Pif1 overexpression in *top3* cells either decreases the length of G2/M and/or increases the chance of survival through G2/M.

Mutant *top3* strains are highly sensitive to the DNA-damaging agents hydroxyurea (HU) and methylmethane sulfonate (MMS). High-copy *PIF1* suppresses these sensitivities in the *top3*Δ strain at low drug concentrations, while at higher concentrations no suppression is evident (Figure 2), consistent with partial suppression of *top3*Δ defects.

Next, we tested the effect of *PIF1* overexpression on the cellular localization of the homologous recombination protein Rad52. Rad52 typically exhibits diffuse nuclear localization but redistributes to discrete foci within the nucleus at sites of DNA double-strand breaks during S phase. These foci are thought to be sites of active DNA repair (LISBY *et al.* 2001, 2003). The majority of the G2/M cells that accumulate in *top3*Δ log-phase cultures each contain a single Rad52 focus, suggesting the presence of DNA damage (data not shown). High-copy Pif1 (p2μ-*PIF1*) does not alter the percentage of unbudded cells that have Rad52 foci in wild-type or *top3*Δ cells (Table 4). Pif1 overexpression also does not affect the percentage of Rad52 foci in wild-type budded cells. However, p2μ-*PIF1* does reduce the incidence of Rad52 foci in *top3*Δ budded cells from 64 to 30%, suggesting that excess Pif1 suppresses the *top3* mutant either by preventing DNA damage or promoting the repair of DNA damage.

Although Pif1 was not recovered in our screen for high-copy suppressors of lethality in the integrated *top3–Y356F* strain, Pif1 overexpression does strongly suppress the lethality caused by *top3–Y356F* overexpression (pGal-*top3–YF*) in a wild-type *TOP3* strain (Figure 3). Galactose-induced expression of *top3–YF*, but not *TOP3*, is toxic, consistent with previous reports (BENNETT and WANG 2001; OAKLEY *et al.* 2002). In contrast, in the presence of galactose, cotransformants of pGal-*top3-YF* and pGal-*PIF1* grow as well as those containing the empty vector controls.

PIF1 gene dosage suppression of *top3* defects is not general to all Pif1 DNA helicase family members. Rrm3, also a 5′ to 3′ DNA helicase, is the closest homolog to Pif1 in *S. cerevisiae* (reviewed in BESSLER *et al.* 2001). Overexpression of *RRM3* (pGal-*RRM3*) does not suppress and, to the contrary, exacerbates *top3*Δ slow growth (data not shown). Similarly, pGal-*RRM3* does not suppress and instead exacerbates the toxicity of *top3–Y356F* overexpression in a wild-type strain background (data not shown).

The requirement of Pif1 catalytic activity for dosage suppression of *top3* defects: To test whether Pif1 helicase activity is necessary for gene dosage suppression of *top3* defects, we substituted arginine for the lysine at amino acid position 264 *(pif1-KR)* in the high-copy *PIF1* vectors. This conserved residue is essential for catalytic activity in all helicases tested (GORBALENYA and KOONIN 1993) and *pif1–K264R* behaves like a null allele *in vivo* (ZHOU *et al.* 2000).

Characterization of pif1-KR overexpression in wild-type cells: Similar to that seen with p2μ-*PIF1*, p2μ-*pif1-KR* slightly lengthens the doubling time of the wild-type strain (W1588-4C) from 156 to 185 min (compare to 181 min for p2μ-*PIF1*), demonstrating a negative effect even in the absence of helicase function. Also similar to p2μ-*PIF1*, p2μ-*pif1-KR* does not affect the cell-cycle profile or Rad52 focus frequency in the wild-type strain (Table 3 and Table 4). There are, however, some differences between *pif1-KR* and *PIF1* overexpression in

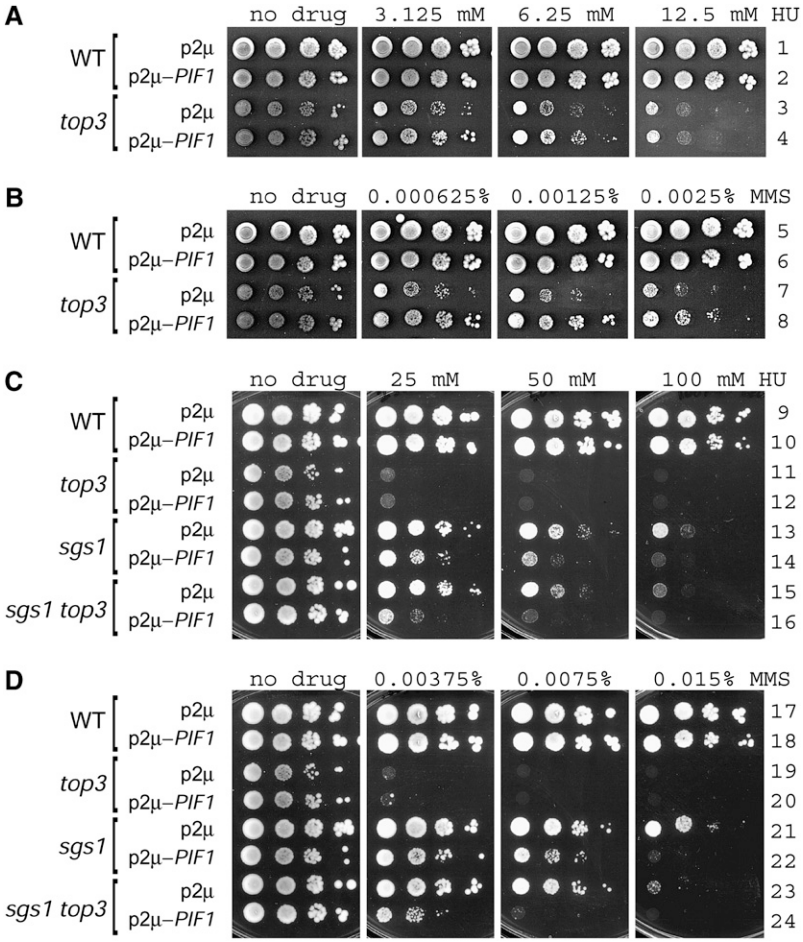

FIGURE 2.—Effect of Pif1 overexpression on HU and MMS sensitivities. Shown are spot assays of 10-fold serial dilutions of wild-type and null mutant strains harboring the indicated plasmids. In each case the most concentrated spot represents 5000 cells. At low concentrations of HU (A) and MMS (B) p2μ-*PIF1* partially suppresses *top3*Δ drug sensitivity. At higher concentrations of HU (C) and MMS (D) p2μ-*PIF1* does not suppress *top3*Δ drug sensitivity and exacerbates *sgs1*Δ and *sgs1*Δ *top3*Δ drug sensitivities. Strains: wild type is W1588-4C; *top3*Δ, *sgs1*Δ, and *sgs1*Δ *top3*Δ are haploid segregants of W1588-4C. Plasmids: p2μ (YEp51B), p2μ-*TOP3* (HCS2), p2μ-*PIF1* (clone 1).

wild-type cells. While p2μ-*PIF1* decreases the wild-type plating efficiency from 100 ± 0.5% to 52 ± 2%, p2μ-*pif1-KR* decreases it only to 72 ± 8%, indicating that *PIF1* toxicity in wild-type cells is partly, but not entirely, due to excess helicase activity. On the other hand, for mitochondria, p2μ-*pif1-KR* has a toxic effect that p2μ-*PIF1* does not exhibit. The frequency of spontaneous petite formation in the wild type (W1588-4C) is 1.1 ± 0.1% and this is increased to 30 ± 3% by p2μ-*pif1-KR*, while p2μ-*PIF1* has little or no effect (0.5 ± 0.1%).

Characterization of pif1-KR overexpression in top3 cells: The p2μ-*pif1-KR* plasmid suppresses defects as well as p2μ-*PIF1* in a *top3*Δ *PIF1* strain background. It also reduces the doubling time of the *top3*Δ *PIF1* cells from 335 to 246 min (compare to 244 min with p2μ-*PIF1*) and partially suppresses the G2/M cell-cycle defect (Table 3) and the frequency of Rad52 foci in budding cells (Table 4). These results might suggest that the mere presence of excess Pif1 protein, and not Pif1 catalytic activity, is important for suppressing *top3*Δ defects. However, we asked whether p2μ-*pif1-KR* could suppress *top3*Δ in the absence of the endogenous chromosomal *PIF1* by assaying pCEN-*TOP3* plasmid loss in a *top3*Δ *pif1*Δ strain transformed with either empty vector, p2μ-*PIF1* or p2μ-*pif1-KR* (see MATERIALS AND METHODS). Only p2μ-*PIF1* was able to suppress the *TOP3* requirement (data not shown). Thus, p2μ-*pif1-KR* does not suppress *top3* defects in a *top3*Δ *pif1*Δ background. These results demonstrate that p2μ-*pif1-KR* cannot suppress *top3*Δ unless at least one functional copy of *PIF1* is present.

Pif1 catalytic activity is required for pGal-*PIF1* suppression of the toxicity associated with *top3–Y356F* overexpression in a wild-type strain (Figure 3). This result further supports the importance of Pif1 catalytic activity for the suppression of *top3* defects. Moreover, cotransformants containing pGal-*top3-YF* and pGal-*pif1-KR* actually fare worse than those containing pGal-*top3-YF* and the empty vector control. The synergy caused by the combination of these two catalytic inactive proteins suggest that Pif1 and Top3 compete for the same substrate (see DISCUSSION).

In addition, our characterization of *pif1-KR* overexpression in the *top3* background demonstrates that gene dosage suppression must be unrelated to Pif1 mitochondrial function. Similar to what was seen in the wild type, in *top3*Δ cells (W1958 segregants), p2μ-*pif1-KR* has a toxic effect on mitochondria with petite formation frequencies of 1.6 ± 0.9%, 1.2 ± 0.5%, and 38.5 ± 2.5% for empty vector, p2μ-*PIF1* and p2μ-*pif1-KR*,

TABLE 4

High-copy *PIF1* suppresses the appearance of DNA repair foci in *top3*Δ cells

Genotype	Vector	% of cells with a Rad52 focus	
		G1[a]	S/G2/M
Wild type	p2μ	0.25[b]	9.7
	p2μ-*PIF1*	0.37	10
	p2μ-*pif1-KR*	1.7	10
*top3*Δ	p2μ	17	64
	p2μ-*PIF1*	17	30
	p2μ-*pif1-KR*	8.1	32

[a] Wild-type (*MAT***a** *TOP3 LYS2 BAR1* segregant from W4436) and *top3*Δ (*MAT***a** *top3*Δ *LYS2 BAR1* segregant from W4436) strains with *RAD52–YFP* integrated at the endogenous locus were transformed with p2μ-*PIF1* (clone 1), p2μ-*pif1-KR* (pWJ1286), or an empty vector (YEp51B) and Rad52 localization was analyzed by fluorescence microscopy. Over 500 cells were viewed for each strain + plasmid background. Cells were categorized for cell-cycle stage as unbudded (G1) or budded (S/G2/M). The cell-cycle distribution for each strain is as follows: Wild type (WT) + p2μ, 63% unbudded and 37% budded; WT + p2μ-*PIF1*, 56% unbudded and 44% budded; WT + p2μ-*pif1-KR*, 54% unbudded and 46% budded; *top3*Δ + p2μ, 34% unbudded and 66% budded; *top3*Δ + p2μ-*PIF1*, 51% unbudded and 49% budded; *top3*Δ + p2μ-*pif1-KR*, 48% unbudded and 52% budded.

[b] Each number represents the percentage of cells in the indicated cell-cycle stage that contain a Rad52–YFP focus.

respectively. Thus p2μ-*PIF1* and p2μ-*pif1-KR* suppress *top3* equally well, despite this negative effect of excess *pif1-KR* on mitochondria. Given these data, as well as our observation that complete mitochondrial deficiency (*rho*^{0}) does not suppress *top3* (data not shown), gene dosage suppression of *top3* defects must, by default, be related to Pif1 nuclear role(s).

The double *pif1 top3* mutant is synthetic lethal in an Sgs1-dependent manner: The genetic interactions among *pif1*Δ, *top3*Δ, and *sgs1*Δ alleles were examined by standard segregation analysis (Figure 4A). No viable *pif1*Δ *top3*Δ haploids were isolated, demonstrating synthetic lethality. *pif1*Δ *top3*Δ spores germinate with wild-type frequency but grow to microcolonies of 2 to 100 swollen large-budded cells suggestive of failure during G2/M. *pif1–K264R top3*Δ is similarly synthetic lethal, demonstrating that Pif1 catalytic activity is required in the absence of Top3 (data not shown). In addition, the *pif1-m2* allele that selectively eliminates nuclear Pif1 is synthetic lethal with *top3*Δ, demonstrating that a nuclear function of Pif1 is important in the absence of Top3 (data not shown). In contrast, *sgs1*Δ *pif1*Δ *top3*Δ and *sgs1*Δ *pif1*Δ segregants are viable and grow as well as the *pif1*Δ mutant alone (Figure 4A). *pif1*Δ, *sgs1*Δ, and *sgs1*Δ *pif1*Δ strains were assayed for HU and MMS sensitivity (Figure 4B and Figure 6D, rows 1–4). The *pif1*Δ strain is mildly sensitive to these drugs compared to the *sgs1*Δ strain. Taking into account the smaller colony size caused by the *pif1*Δ petite phenotype, the *sgs1*Δ *pif1*Δ double mutant resembles the *sgs1*Δ mutant. These results indicate that there is no *sgs1*Δ *pif1*Δ synthetic interaction. Taken together, these genetic analyses reveal that Pif1 DNA helicase activity is essential for dealing with nuclear DNA damage that arises in the *top3* mutant strain when Sgs1 is present.

The genetic interaction of Pif1 with the Sgs1–Top3 pathway is not a general property of the Pif1 DNA helicase family. The *rrm3*Δ *top3*Δ combination is synthetic lethal; however, this lethality is not suppressed by *sgs1*Δ. (data not shown). Furthermore, in agreement with previous reports, the *sgs1*Δ *rrm3*Δ combination is inviable (Tong *et al.* 2001; Ooi *et al.* 2003; Schmidt and Kolodner 2004; Torres *et al.* 2004).

Sgs1 catalytic activity is required for Pif1–Top3 genetic interactions: We further examined the effects of *sgs1*Δ as well as other several *sgs1* mutations, on Pif1–Top3 genetic interactions. The *sgs1-*Δ*N82* mutation deletes the N terminus of Sgs1 that physically interacts with Top3, mimicking a *top3* mutation even in the presence of wild-type *TOP3* (Duno *et al.* 2000; Fricke *et al.* 2001). The *sgs1-K706R* (*sgs1-KR*) mutation eliminates Sgs1 helicase activity by substituting arginine for the conserved lysine at amino acid position 706 (Lu *et al.* 1996).

*sgs1*Δ suppresses many *top3* defects, including slow growth and sensitivity to HU and MMS. Both *sgs1*Δ and

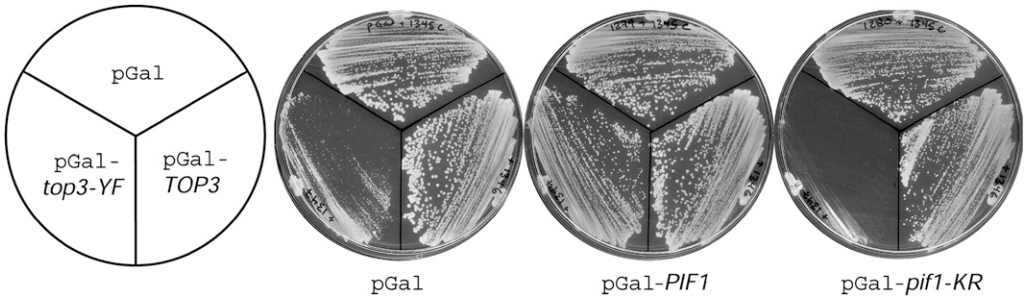

Figure 3.—Toxicity caused by overexpression of the catalytically inactive Top3 protein is suppressed by overproduction of Pif1. Pictured are galactose plates on which wild-type strains (W1588-4C) cotransformed with the indicated plasmids have been streaked (see materials and methods). The empty vector controls are designated pGal. Galactose-induced expression of *top3–Y356F* but not *TOP3* is toxic. pGal-*PIF1* strongly suppresses pGal-*top3-YF* toxicity. In contrast, co-expression of pGal-*pif1–KR* does not suppress and instead exacerbates pGal-*top3-YF* toxicity. Top3 plasmid series is *HIS3*-marked: pGal (pWJ1345), pGal-*TOP3* (pWJ1346), pGal-*top3-YF* (pWJ1347). Pif1 plasmid series is *URA3*-marked: pGal (pWJ1047), pGal-*PIF1* (pWJ1279), pGal-*pif1-KR* (pWJ1280).

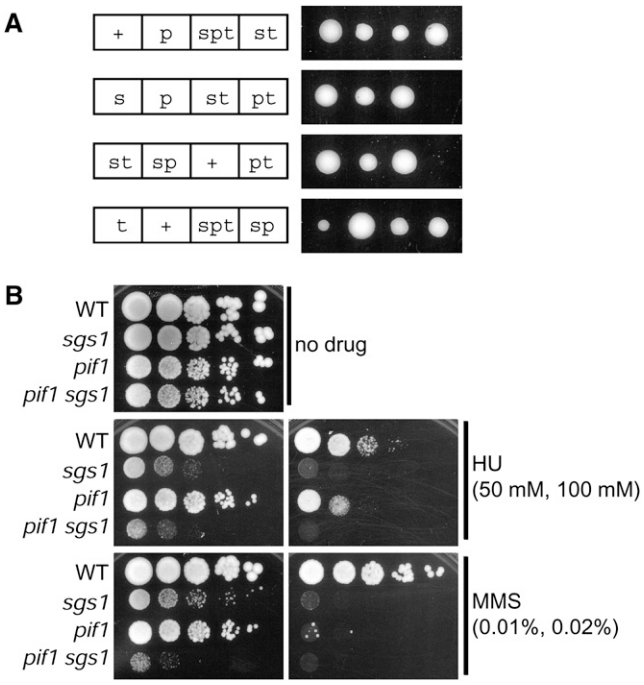

FIGURE 4.—*pif1 top3* is synthetic lethal in an Sgs1-dependent manner. (A) Four representative tetrads segregated from a *sgs1*Δ *pif1*Δ *top3*Δ heterozygous diploid (W3642) are shown. The genotype of each segregant is indicated: wild type (+), *pif1*Δ (p), *sgs1*Δ (s), *top3*Δ (t). The dead *pif1*Δ *top3*Δ segregants (pt) appear as microcolonies and do not grow further upon restreaking of the spore colony. (B) HU and MMS sensitivity of wild-type (W1588-4C) and *pif1*Δ, *sgs1*Δ, and *sgs1*Δ *pif1*Δ segregants (W3642). Tenfold serial dilutions were spotted on YPD or YPD plates containing 50 mM HU (left), 100 mM HU (right), 0.01% MMS (left), or 0.02% MMS (right). In each case, the most concentrated spot represents 50,000 cells.

*sgs1*Δ *top3*Δ strains are mildly sensitive to HU and MMS and p2μ-*PIF1* does not suppress but, to the contrary, exacerbates these drug sensitivities (Figure 2). These results indicate that Pif1 interaction with the Sgs1–Top3 pathway is specific to DNA damage that arises when Sgs1 acts in the absence of Top3.

In the *sgs1-ΔN82* strain, p2μ-*PIF1* partially suppresses slow growth (Figure 5A) and MMS sensitivity (Figure 5B, rows 7 and 8). In contrast, when Sgs1 catalytic activity is eliminated in the context of this mutation (*sgs1-ΔN82, KR*) p2μ-*PIF1* compromises growth (Figure 5A) and increases MMS drug sensitivity (Figure 5B, rows 9 and 10). These results corroborate that Pif1 overexpression is beneficial specifically when Sgs1 helicase activity is uncoupled from Top3.

sgs1-KR suppresses *pif1*Δ *top3*Δ lethality, demonstrating that the *pif1*Δ *top3*Δ synthetic interaction is due to Sgs1 helicase activity (Figure 6A). We next looked for genetic interactions between the different *sgs1* mutant alleles and *pif1*Δ in a wild-type *TOP3* background. The *sgs1-ΔN82 pif1*Δ combination is synthetic lethal and this is suppressed by removal of Sgs1 catalytic activity (*sgs1-ΔN82, KR*) (Figure 6B and 6C). Taking into account the smaller colony size caused by the *pif1*Δ petite phenotype, both the *pif1*Δ *sgs1-KR* and *pif1*Δ *sgs1-ΔN82, KR* double mutants exhibit growth and MMS sensitivity similar to the respective *sgs1* single mutants (Figure 6D, rows 5–8). Thus the synthetic interaction between *pif1*Δ and the Sgs1–Top3 pathway also occurs specifically when Sgs1 helicase activity is uncoupled from Top3.

Taken together, these genetic analyses strongly suggest that Pif1 is important when the Sgs1 DNA helicase creates a substrate that is not accessible to resolution by the Top3 topoisomerase (see DISCUSSION).

The Pif1–Top3 genetic interaction is recombination dependent: Eliminating homologous recombination suppresses the *top3* growth defect (OAKLEY *et al.* 2002; SHOR *et al.* 2002). We found that p2μ-*PIF1* does not suppress *rad52 top3* or *rad52* slow growth, consistent with the notion that *PIF1* high-copy suppression of *top3* defects does not occur in the absence of homologous recombination (data not shown). In addition, *rad51*Δ, *rad52*Δ, *rad54*Δ, or *rad55*Δ deletions suppress the *pif1*Δ *top3*Δ synthetic defect, demonstrating that *pif1*Δ *top3*Δ synthetic lethality is recombination dependent (Figure 7 and data not shown). Neither *rad9* nor *mad2* mutation suppresses *pif1*Δ *top3*Δ, indicating that the synthetic defect is independent of the DNA damage and spindle checkpoints (data not shown). We found that the *top3*Δ *rrm3*Δ and *sgs1*Δ *rrm3*Δ synthetic interactions are similarly recombination dependent and checkpoint independent (data not shown).

sgs1, *top3*, *sgs1 top3*, *pif1*, and *rrm3* mutants had different effects on recombination between repeated sequences. Three distinct repetitive loci, *CUP1*, rDNA, and *SUP4*, were examined. The *sgs1* and *top3* mutations cause hyperrecombination at all three loci (Table 5 and WALLIS *et al.* 1989; SHOR *et al.* 2002). Mutation of *rrm3* causes hyperrecombination at rDNA and *CUP1* (Table 5 and KEIL and MCWILLIAMS 1993), but has no effect at the *SUP4* locus (Table 5). Mutation of *pif1* causes hyperrecombination at *CUP1* and *SUP4*, but has little effect at the rDNA locus (Table 5). Thus, while *sgs1* and *top3* appear to have a general effect on recombination between repeated sequences, *pif1* and *rrm3* have locus-specific effects that differ from each other. These results corroborate that Pif1 and the Sgs1–Top3 pathway do not share a global common function and are consistent with Pif1 and Rrm3 also having distinct functions.

Pif1 localizes to DNA repair foci in *top3* mutant cells: Pif1 localization was studied in live cells using a Pif1–YFP fusion protein. *PIF1–YFP* exhibits no synthetic interaction with *top3*Δ and no associated mitochondrial deficiency, demonstrating that it produces functional Pif1 protein (data not shown). We found that Pif1 is present in the mitochondria as seen by colocalization with the mitochondrial protein Cox4 (Figure 8A). Pif1 also exhibits nuclear localization and is largely concentrated in the nucleolus as evidenced by colocalization studies

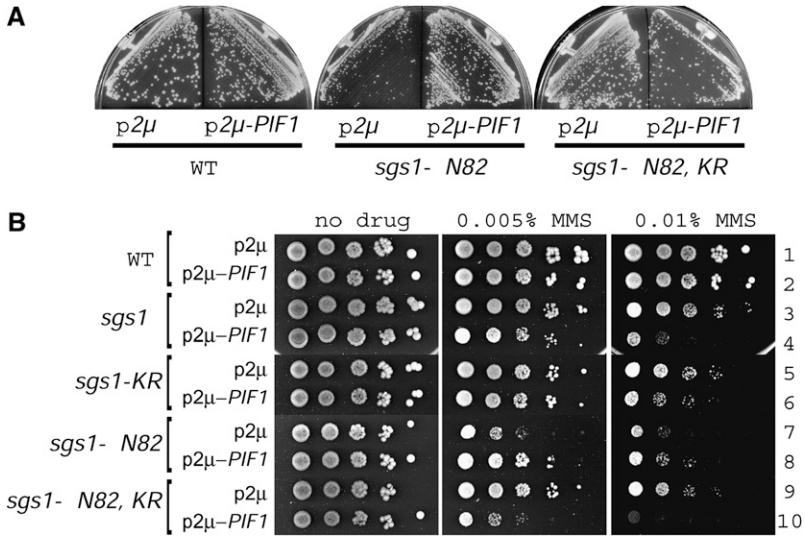

FIGURE 5.—The effect of Pif1 overexpression in different *sgs1* allelic backgrounds. (A) The indicated *sgs1* strains containing either empty vector (p2μ) or high-copy Pif1 (p2μ-*PIF1*) were streaked on SC-Leu plates and incubated for 3 days. (B) Wild-type and *sgs1* mutants containing p2μ or p2μ-*PIF1* were tested for sensitivity to HU and MMS. Shown are 10-fold serial dilutions on SC-Leu containing the indicated concentration of drug. The most concentrated spot in each case represents 50,000 cells. Strains: wild type (W1588-4C), *sgs1*Δ (W1958 segregant), *sgs1-*Δ*N82* (W2069-2B), *sgs1-KR* (W1911-1B), *sgs1-*Δ*N82,* (W2075-3C). Plasmids: p2μ (YEp51B), p2μ-*PIF1* (Clone 1).

with the nuclear membrane marker Nup49 and the nucleolar protein Nop1 (Figure 8B). Occasionally, Pif1 spontaneously redistributes to a single nuclear focus that is outside of the nucleolus. These spontaneous Pif1 foci are rare in G1 (0.6%) cells, but increase in frequency as cells enter the S (7%) and G2/M (12%) phases of the cell cycle (Table 6). These results suggest that Pif1 is recruited to nuclear foci during DNA replication and/or chromosome segregation.

Colocalization studies with Rad52–CFP revealed that almost all nuclear Pif1 foci (>96%) colocalize with a Rad52 focus at all phases of the cell cycle (Table 6).

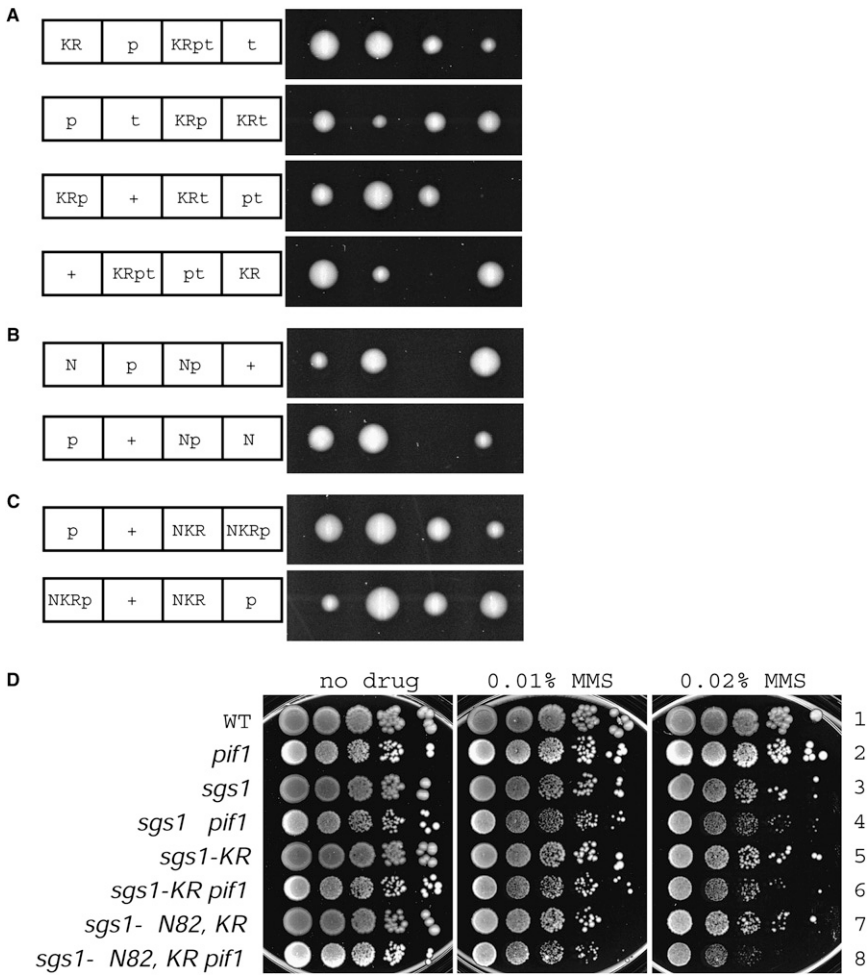

FIGURE 6.—The interaction of *pif1*Δ with different *sgs1* alleles. (A) *pif1*Δ *top3*Δ synthetic lethality is suppressed by the *sgs1-K706R* catalytic inactive allele. Four representative tetrads from segregation of a *sgs1-K706R pif1*Δ *top3*Δ heterozygote (W5497) are shown: wild type (+), *sgs1-K706R* (KR), *pif1*Δ (p), *top3*Δ (t). (B) Deletion of the Top3 interaction domain in Sgs1 (*sgs1-*Δ*N82*) is synthetic lethal with *pif1*Δ. Two representative tetratypes from a *sgs1-*Δ*N82 pif1*Δ heterozygote (W5493) are shown: wild type (+), *sgs1-*Δ*N82* (N), *pif1*Δ (p). (C) *sgs1-*Δ*N82 pif1*Δ synthetic lethality is suppressed by the elimination of Sgs1 catalytic activity (*sgs1-*Δ*N82, K706R*). Two representative tetratypes from a *sgs1-*Δ*N82, K706 pif1*Δ heterozygote (W5495) are shown: wild type (+), *sgs1-*Δ*N82, K706R* (NKR), *pif1*Δ (p). (D) MMS sensitivity of viable segregants from the above crosses. Tenfold serial dilutions were spotted on SC-Leu plates with or without drug. The most concentrated spot in each case has 50,000 cells. Strains: wild type (W1588-4C), *pif1*Δ (W5388 segregant), *sgs1*Δ (W1958 segregant), *sgs1*Δ *pif1*Δ (W5489 segregant), *sgs1-KR* (W5491 segregant), *sgs1-KR pif1*Δ (W5491 segregant), *sgs1-*Δ*N82, KR* (W5495 segregant), *sgs1-*Δ*N82, KR pif1*Δ (W5495 segregant).

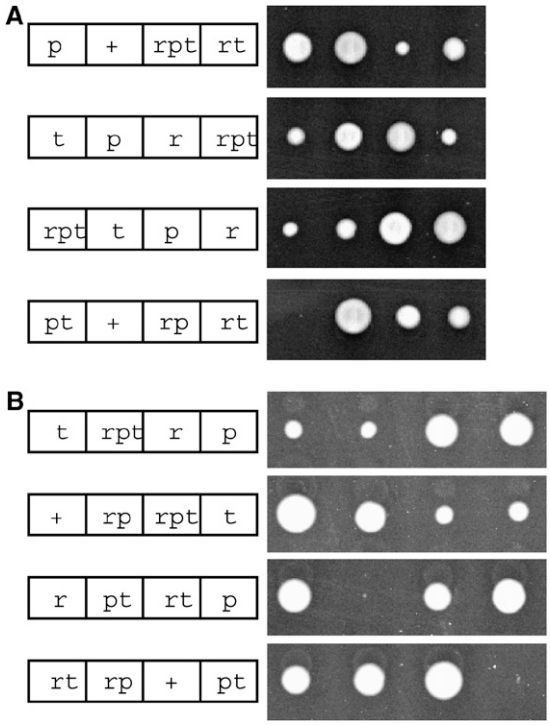

FIGURE 7.—Eliminating homologous recombination suppresses *pif1 top3* synthetic lethality. (A) *rad54* deletion suppresses *pif1 top3* lethality. Four representative tetrads from the segregation of a *rad54*Δ *pif1*Δ *top3*Δ heterozygous diploid (W3688) are shown: wild type (+), *rad54*Δ (r), *pif1*Δ (p), *top3*Δ (t). (B) *rad55* deletion suppresses *pif1 top3* lethality. Four representative tetrads from the segregation of a *rad55*Δ *pif1*Δ *top3*Δ heterozygous diploid (W3689) are shown: wild type (+), *rad55*Δ (r), *pif1*Δ (p), *top3*Δ (t). Similar results were obtained with *rad51* and *rad52* deletions (not shown).

Conversely, only a subset of the Rad52 foci colocalize with a Pif1 focus (35% during S phase and 77% during G2/M phase). The extent of Pif1 and Rad52 focus colocalization was unaffected by strain background (*top3* mutant *vs.* wild type) or cell treatment (ionizing radiation). Overall, more spontaneous Pif1 foci are detected in G2/M cells and the extent of Pif1 focus colocalization with Rad52 is highest in G2/M cells. This may suggest that recruitment of Pif1 to the DNA repair focus is a relatively late event that occurs after Rad52 recruitment. However, Pif1 foci still form in a *rad52*Δ strain and Rad52 foci still form in a *pif1*Δ strain, indicating that Pif1 and Rad52 can participate in independent DNA repair pathways (data not shown).

Ionizing radiation causes DNA double-strand breaks and induces Rad52 focus formation in budding cells (LISBY *et al.* 2001). We asked whether Pif1 nuclear foci are similarly induced. Cells were exposed to 4 krad, a gamma ray dose that gives two DNA double-strand breaks per cell on average (LISBY *et al.* 2001) and monitored Rad52–YFP and Pif1–CFP focus formation for 3 hr postirradiation (Figure 8D). The percentage of unbudded (G1) cells with a Rad52 (4.2%) or Pif1 (3.1%) focus was low and remained relatively constant over the course of the experiment. Consistent with previously published results (LISBY *et al.* 2001), the frequency of budded (S/G2/M) cells with a Rad52 focus increased from 19% pre-irradiation to 85% at 150- and 180-min postirradiation. The frequency of budded cells with a Pif1 nuclear focus paralleled what was seen for Rad52, increasing from 9.5% pre-irradiation to 66% at 150- and 180-min postirradiation. These results suggest that Pif1 foci form in response to DNA double-strand breaks caused by gamma irradiation. However, a *pif1*Δ strain is not sensitive to 80 krad, the highest gamma ray dose tested, demonstrating that Pif1 is not required to survive this type of DNA damage.

Strikingly, in the *top3*Δ strain, the incidence of spontaneous Pif1 foci increases to 18% in S-phase cells (from 7% in the wild type) and 66% in G2/M cells (from 12% in the wild type) (Table 6 and Figure 8E). Except for the increased frequency of Pif1 foci in these *top3* mutant cells, Pif1 localization appears wild type (Figure 8). Pif1 localization and the frequency of Pif1 nuclear foci in *sgs1*Δ and *sgs1*Δ *top3*Δ strains are similar to what is observed in the wild-type strain (data not shown). Taken together, these data suggest that the increased frequency of Pif1 recruitment to DNA repair foci in *top3* cells must be due to DNA damage that occurs when Sgs1 acts in the absence of Top3.

In contrast to our results with Pif1 localization, a functional Rrm3–YFP fusion protein did not form visible foci in wild-type, *sgs1*Δ, or *top3*Δ cells. This suggests that the ability to form a nuclear focus is not general to this family of DNA helicases but is specific to Pif1.

DISCUSSION

While it is clear that Sgs1 and Top3 work together in a pathway that promotes genome stability, their cellular DNA substrate(s) remains an area of intense investigation. Previous genetic screens designed to provide clues to Sgs1–Top3 function have included searches for mutations that are synthetic lethal in combination with *sgs1* (MULLEN *et al.* 2001; TONG *et al.* 2001; OOI *et al.* 2003; SCHMIDT and KOLODNER 2004; TORRES *et al.* 2004) and searches for mutational suppressors of *top3* mutant slow growth (GANGLOFF *et al.* 1994b; SHOR *et al.* 2002). Genes that synthetically interact with *sgs1* include *srs2*, *rrm3*, and members of the *mus81-mms4*, *slx5-slx8*, and *slx1-slx4* heterodimeric complexes. Mutations in these genes are also synthetic lethal with *top3*, indicating that these gene products likely act in pathways that have functional overlaps with the Sgs1–Top3 pathway. An exhaustive search for mutational suppressors of *top3* slow growth identified, in addition to *sgs1*, members of the *RAD52* epistasis group of proteins required for homologous recombination, contributing to the idea that Sgs1–Top3 is involved in the resolution of recombination intermediates (SHOR *et al.* 2002).

TABLE 5

Recombination frequencies at the *CUP1*, rDNA, and *SUP4*-o loci

	CUP1[a]: 5-FOA^R/total $\times 10^6$	rDNA[b]: 5-FOA^R/total $\times 10^5$	*SUP4*-**o**[c]: 5-FOA^R Ade$^-$ Can^R/total $\times 10^7$
WT	3.7 ($\pm$ 0.96)[d]	16 ($\pm$ 3.8)	2.1 ($\pm$ 1.1)
pif1[e]	88 ($\pm$ 12)	29 ($\pm$ 6.6)	16 ($\pm$ 7.1)
rrm3	100 ($\pm$ 27)	140 ($\pm$ 66)	4.3 ($\pm$ 3.2)
sgs1	78 ($\pm$ 6.1)	130 ($\pm$ 28)	25 ($\pm$ 6.1)
top3	188 ($\pm$ 43)	220 ($\pm$ 71)	180 ($\pm$ 47)
sgs1 top3	84 ($\pm$ 26)	40 ($\pm$ 24)	46 ($\pm$ 6.4)

[a] The *CUP1* locus consists of six to seven 2.0-kb direct repeats in the assay strain (W1588-4C background) as determined by gel blot analysis and phosphorimager quantitation (data not shown).

[b] The rDNA locus contains 150–200 9.2-kb direct repeats in tandem as well as a replication fork barrier in each repeat.

[c] The *SUP4*-**o** locus contains five ~330-bp δ repeats in both direct and inverse orientations as well as replication pause sites (Rothstein *et al.* 1987).

[d] See materials and methods for details of how each assay was performed. Each value represents the deletion frequency between direct repeats at the indicated locus and is the average of a minimum of five experiments in which independent segregants were used. Standard deviations are given in parentheses.

[e] Null mutant strains were used except in the case of the *SUP4*-**o** assay in which case the *pif1-m2* strain was used for technical reasons (see materials and methods). Strains used in this analysis were constructed by crossing the appropriate mutation into the appropriate assay strain: W3831-1B (*CUP1* assay), W3480-4C (rDNA assay), or W1868-8B (*SUP4*-**o** assay). The *sgs1* and *top3* deletions were derived from a W1958 segregant. The *pif1* deletion was derived from strain J1129. The *pif1-m2* mutation was derived from strain W3972-7C. The *rrm3* deletion was derived from strain J1132.

A current model to explain RecQ–Topo III biology suggests that RecQ creates a DNA substrate that is resolved by Topo III. Furthermore, it appears that RecQ helicase activity is toxic in the absence of Topo III, since Topo III mutant defects are suppressed by mutation of RecQ homologs in budding and fission yeasts (Gangloff *et al.* 1994a; Murray *et al.* 1997; Stewart *et al.* 1997). In *S. cerevisiae*, a catalytically inactive *top3* allele causes a more severe phenotype than the null allele and is also suppressed by *sgs1*, suggesting that the catalytically inactive Top3 protein binds to and stabilizes a toxic Sgs1-created substrate. *In vivo* and *in vitro* data support the notion that RecQ–Topo III is involved in the resolution of recombination intermediates at the end of DNA replication (reviewed in Heyer *et al.* 2003). We presume that the toxic DNA structure that persists in *top3* mutants is a normally transient recombination intermediate of the Sgs1–Top3 pathway that arises during DNA replication.

The Pif1 DNA helicase genetically interacts with the Sgs1–Top3 pathway: Here, we show that high-copy Pif1 can suppress *top3* mutant defects (Figures 1–3 and Tables 3–4) and that the *pif1 top3* mutant combination is synthetic lethal (Figure 4). Furthermore, our data demonstrate that these interactions between Pif1 and the Sgs1–Top3 pathway are specific to the condition that occurs when Sgs1 is uncoupled from Top3. High-copy Pif1 does not suppress *sgs1*Δ or *sgs1*Δ *top3*Δ defects and even makes these strains more sensitive to DNA damaging agents (Figure 2C–2D). Furthermore, *sgs1*Δ suppresses *pif1*Δ *top3*Δ synthetic lethality and *pif1*Δ *sgs1*Δ mutants have no synthetic defect (Figure 4). These observations indicate that Pif1 and Sgs1 do not share a common function, which is not surprising given the opposite polarities of their helicase activities. Our results also demonstrate that Pif1 overexpression does not alleviate the need for the Sgs1–Top3 pathway. Rather, our data are consistent with Pif1 being required to deal with a toxic DNA structure that is created by Sgs1 and that accumulates when Top3 is absent.

Pif1 helicase activity is required to counteract Sgs1 helicase activity in the absence of Top3: Pif1 helicase activity is important for the interaction of Pif1 with the Sgs1–Top3 pathway. In the complete absence of wild-type Pif1 (*top3*Δ *pif1*Δ strains), high-copy *pif1-KR* cannot suppress *top3* defects, demonstrating that some Pif1 catalytic activity, provided by at least one copy of *PIF1*, is essential for the suppression of *top3* defects. Pif1 catalytic activity is also required for gene dosage suppression of the toxicity caused by *top3-YF* overexpression in a wild-type strain (Figure 3). Furthermore, in *top3* mutants, Pif1 catalytic activity becomes essential as evidenced by *top3 pif1–K264R* synthetic lethality. Together, these results establish that Pif1 helicase activity is absolutely required to promote survival in the absence of Top3.

We also show that the interaction of Pif1 with the Sgs1–Top3 pathway manifests specifically when Sgs1 helicase activity is uncoupled from Top3. For example, in the absence of Sgs1 catalytic activity (*sgs1–K706R top3* and *sgs1–K706R* mutants), Pif1 overexpression is no longer beneficial and is instead toxic (Figure 5B,

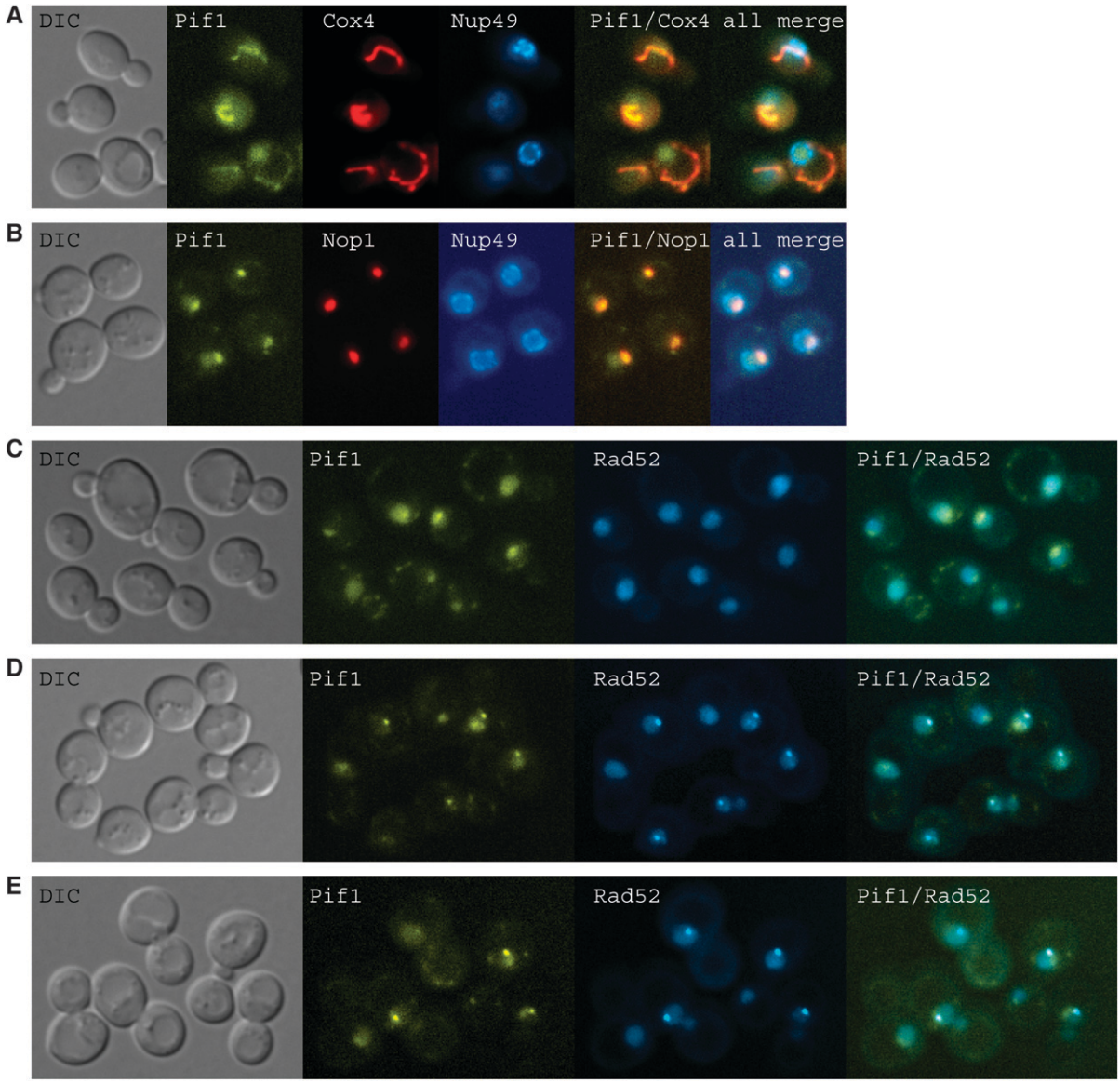

Figure 8.—Cellular localization of Pif1. The Pif1 protein is tagged with *YFP* via integration of the *YFP* epitope at the endogenous *PIF1* locus. In all cases a Z-stack of 13 sections was taken such that the entire volume of each cell was analyzed. In A–E, the section that best emphasizes what is intended is pictured. (A) Pif1 is found in mitochondria as evidenced by colocalization with the mitochondrial marker Cox4. For reference, the position of the nucleus is indicated by Nup49, a nuclear membrane protein. Strain: W4180-8D (Pif1–YFP). Plasmids: pWJ1326 (Cox4–DsRed) and pWJ1348 (CFP–Nup49). (B) Pif1 is found in the nucleus with a pronounced concentration in the nucleolus as evidenced by colocalization with the nuclear marker Nup49 and nucleolar marker Nop1. Strain: W4180-8D (Pif1–YFP). Plasmids: pWJ1323 (Nup49–CFP) and pWJ1322 (Nop1–DsRed). (C–E) Pif1 occasionally localizes to discrete nuclear foci that correspond to Rad52 DNA repair foci. These Pif1 foci are induced by gamma irradiation and found with increased incidence in *top3* mutant cells. Pif1 and Rad52 colocalization is shown in wild-type cells (C), in wild-type cells 1-hr after 4 krad of gamma rays (D) and in *top3*Δ cells (E). Strains: W4240-25B (*PIF1–YFP RAD52–CFP*) and haploid segregants of W4238 (*top3*Δ *PIF1–YFP RAD52–CFP*).

rows 5 and 6 and data not shown). Additionally, while an *sgs1* mutation that does not physically interact with Top3 and mimics a *top3* phenotype (*sgs1-ΔN82*) is suppressed by Pif1 overexpression, eliminating Sgs1 catalytic activity in this context (*sgs1-ΔN82, K706R*) renders excess Pif1 toxic (Figure 5A and 5B, rows 7–10). Thus, Pif1 gene dosage suppression of *top3* defects is dependent upon an active Sgs1 helicase. Similarly, *pif1 top3* synthetic lethality is evident only when the Sgs1 helicase is active since it is suppressed by introducing the *sgs1–K706R* mutation (Figure 6A). Consistent with this observation, the synthetic lethality of *sgs1-ΔN82 pif1* is suppressed when the helicase activity of *sgs1-ΔN82* is eliminated *(sgs1-ΔN82, K706R*) (Figure 6B and 6C). These results demonstrate that Sgs1 helicase activity that is uncoupled from Top3 is lethal in cells that lack

TABLE 6

Pif1 localizes to DNA repair foci

Genotype[a]	Cell-cycle stage		
	G1	S	G2/M
Wild type			
% of cells with a Rad52 focus	0.9[c]	22	16
% of cells with a Pif1 focus[b]	0.6	7	12
*top3*Δ			
% of cells with a Rad52 focus	3	46	84
% of cells with a Pif1 focus[c]	2	18	66

[a] Over 700 cells were examined for each genotype. Results are compiled from at least three different wild-type (*TOP3 RAD52–CFP PIF1–YFP*) and three different *top3*Δ (*top3::TRP1 RAD52–CFP PIF1–YFP*) haploid segregants from strain W4238. The cell-cycle distribution for wild type is 49% G1, 25% S, and 26% G2/M. The cell-cycle distribution for *top3*Δ is 38% G1, 18% S, and 44% G2/M.

[b] For both wild type and *top3*Δ, S and G2/M Pif1 foci colocalize with Rad52 foci >96% of the time; for both wild type and *top3*Δ, Rad52 foci colocalize with Pif1 foci 35% of the time during S phase and 77% of the time during G2/M phase.

[c] Percentage of cells in the indicated cell-cycle stage that contain a nuclear focus is presented.

Pif1. Taken together, our results establish that Pif1 helicase activity is essential to counteract Sgs1 helicase activity and promote survival in the absence of Top3.

Known roles of Pif1 cannot account for its genetic interaction with the Sgs1–Top3 pathway: Roles ascribed to Pif1 to date include maintenance of rDNA and regulation of telomerase-dependent DNA replication (Schulz and Zakian 1994; Ivessa *et al.* 2000; Zhou *et al.* 2000; Mangahas *et al.* 2001; Myung *et al.* 2001). We found that deletion of the rDNA tandem array does not suppress *pif1 top3* synthetic lethality or *top3* slow growth (data not shown). We also found that mutations that eliminate telomerase-dependent telomere replication (*e.g.*, *est2* or *ku70*) (Myung *et al.* 2001) do not suppress *pif1 top3* synthetic lethality or *top3* slow growth (data not shown). These results demonstrate that the genetic interaction between Pif1 and the Sgs1–Top3 pathway is unrelated to the roles of Pif1 in rDNA maintenance and at telomeres. Thus Pif1 must have additional nuclear functions that account for the *pif1 top3* genetic interaction.

The work presented here indicates a broader role for Pif1 in maintenance of nuclear genome integrity. Previous studies showed that lack of Pif1 does not affect chromosome loss, reciprocal recombination, or gene conversion (Schulz and Zakian 1994). However, at *CUP1* and *SUP4*, two repetitive loci outside of the rDNA array, we find that *pif1* mutants are hyperrecombinant, suggesting that Pif1 has a general role in the maintenance of repeated sequences (Table 5). We also examined *pif1* mutants for sensitivity to several DNA damaging agents including HU that leads to stalled replication forks, gamma rays that create dsDNA breaks, and MMS that creates alkylated DNA adducts that are likely processed to dsDNA breaks. Although *pif1* null mutants are mildly sensitive to HU (Figure 4B), otherwise wild-type cells that lack mitochondria (*rho*^{0}) exhibit similar sensitivity, suggesting that *pif1* HU sensitivity is due to its mitochondrial defect (unpublished). *pif1* cells are MMS sensitive (Figure 4B) while *rho*^{0} cells are not (unpublished), demonstrating that nuclear Pif1 provides protection against MMS-induced DNA damage. In contrast, *pif1* mutants are not gamma ray sensitive (RESULTS and data not shown). These observations indicate that there is something specific to the type of damage induced by MMS that calls for Pif1 and not the presence of dsDNA breaks *per se*. Interestingly, *top3* mutants are also highly MMS sensitive but not gamma ray sensitive (unpublished), suggesting an overlapping role for Pif1 and Top3 in dealing with certain types of DNA damage.

The role of Pif1 in the Sgs1–Top3 pathway is downstream of recombination: Several lines of evidence place the essential role of Pif1 in *top3* mutants downstream of homologous recombination. While high-copy Pif1 suppresses a *top3* mutant, it does not suppress the slow growth of *rad52 top3* double mutants, suggesting that Pif1 gene dosage suppression of *top3* defects does not occur in the absence of recombination. Even more convincing, *pif1 top3* synthetic lethality is suppressed by deleting members of the Rad52 epistasis group of homologous recombination genes, demonstrating that the lethal event in *pif1 top3* strains occurs downstream of recombination (Figure 7). These results indicate that the genetic interaction of Pif1 with the Sgs1–Top3 pathway is recombination dependent.

We find that the majority of G2/M cells that accumulate in a *top3* culture contain a single Rad52 DNA repair focus, corroborating the idea that Sgs1 creates a toxic recombination intermediate that persists at the end of DNA replication in *top3* mutants. Pif1 overexpression suppresses both the cell-cycle defect and the increased frequency of DNA repair foci in *top3* mutants, suggesting that the mechanism of suppression is related to prevention, resolution, or repair of stalled recombination intermediates in *top3* mutants (Table 3 and Table 4). Furthermore, when we examined Pif1 cellular localization, we found that Pif1 itself localizes to the frequent DNA repair foci found in *top3* mutant budding cells (Figure 8 and Table 6). While 35% of Rad52 foci in *top3* mutant S-phase cells contain Pif1, this number increases to 77% in G2/M cells, suggesting that Pif1 localization to the DNA repair center is a late event. These data are consistent with a scenario in which Pif1 is recruited to DNA repair centers in *top3* mutant cells to deal with toxic DNA structures created by Sgs1.

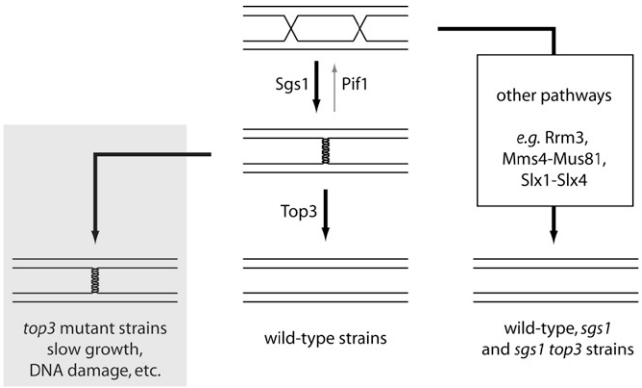

Figure 9.—A model for the genetic interaction between Pif1 and Sgs1–Top3. Pif1 interacts with the Sgs1–Top3 pathway downstream of homologous recombination. A concerted Sgs1–Top3 activity is proposed to be one means of resolving recombination intermediates at the end of DNA replication, such as the double Holliday junction that is pictured (Heyer *et al.* 2003). In this Sgs1–Top3 resolvase model, Sgs1 molecules act on opposing DNA strands to convergently branch migrate the Holliday junctions, forming a hemicatenated strand interlink that is resolved by Top3 (middle). In the absence of Top3, the Sgs1-created substrate persists, is not efficiently resolved by other pathways, and is toxic to the cell as evidenced by the myriad defects of *top3* mutants (shaded box). In the absence of Sgs1 (*sgs1* or *sgs1 top3* strains), this toxic substrate is never created, leaving the recombination intermediate accessible to alternative pathways (white box). Our results demonstrate that Pif1 helicase activity is required to counteract Sgs1 helicase activity that has become uncoupled from Top3. Our data suggest that Pif1 either reverses or prevents formation of this detrimental Sgs1-created DNA structure.

What is the mechanism by which Pif1 helicase activity suppresses toxicity caused by Sgs1 in the absence of Top3? An emerging theme has been that RecQ–Topo III is important for processing recombination intermediates that form during DNA replication (reviewed in Heyer *et al.* 2003). Double Holliday junctions are a proposed intermediate in the repair of collapsed replication forks as well as in the postreplication repair of gaps left as the replication fork bypasses DNA lesions. Classically, Holliday junctions are thought to be resolved by a resolvase activity that yields a recombinogenic crossover event half of the time. *In vitro* studies demonstrate a concerted Blm–Topo IIIα activity that resolves double Holliday junctions without crossing over and *in vivo* evidence in yeast suggests that Sgs1–Top3 possesses a similar activity (Ira *et al.* 2003; Wu and Hickson 2003; Wu *et al.* 2005). In the current model for Sgs1–Top3 resolvase activity, Sgs1 molecules act on opposing DNA strands to branch migrate two Holliday junctions toward each other, creating a hemicatenated strand interlink between two chromosomes that is a substrate for decatenation by Top3 (central panel in Figure 9 and reviewed in Heyer *et al.* 2003). In the absence of Sgs1 (*sgs1* and *sgs1 top3* strains), pathways that act in parallel provide alternate means of resolution (white box in Figure 9). In the absence of Top3, Sgs1 molecules act on the double Holliday junction to create a DNA structure that persists and causes characteristic *top3* mutant defects (shaded box in Figure 9). Our results clearly demonstrate that Pif1 helicase activity is required to counteract Sgs1 helicase activity in *top3* mutants.

How does Pif1 counteract Sgs1 activity? One possibility is that Pif1 strips Sgs1 protein from DNA, thus preventing the cell from committing to a defunct repair pathway in *top3* mutants. Such a role in protein removal from DNA has been described for the Srs2 DNA helicase in disassembly of Rad51 filaments (Krejci *et al.* 2003; Veaute *et al.* 2003). Another possibility is that Pif1 recognizes and rewinds a toxic DNA substrate created by Sgs1, leaving it accessible to repair by other pathways. Consistent with this idea, Sgs1 and Pif1 unwind DNA with opposing polarities and Pif1 activity is stimulated by forked DNA structures (Lahaye *et al.* 1991; Lahaye *et al.* 1993; Bennett *et al.* 1998, 1999). Here, we show that Sgs1 helicase activity is required for the genetic interaction of Pif1 with Sgs1–Top3, and this lends credence to the idea that the Sgs1-created DNA substrate *per se* is important for the interaction. In further support of the idea that Pif1 acts on an Sgs1-created substrate, we show that excess *pif1-KR* suppresses *top3* defects in cells with at least a single copy of Pif1 (*top3 PIF1*) but not in *top3 pif1* cells, suggesting that as long as some functional Pif1 is present, the catalytically inactive protein stabilizes/protects the substrate for Pif1 until a functional Pif1 arrives to act at the site. Consistent with this idea, Pif1 does exhibit distributive activity *in vitro* with the protein readily binding/releasing its substrate (Lahaye *et al.* 1993).

These two proposed roles for the requirement of Pif1 in *top3* mutants, removal of Sgs1 protein from its DNA substrate by Pif1 *vs.* the active rewinding of an Sgs1-created substrate by Pif1, are not necessarily mutually exclusive. It is also possible that Sgs1 normally remains bound at the ssDNA–dsDNA junction after DNA unwinding (branch migration) until Top3 arrives and that mere removal of Sgs1 from the DNA at this point permits passive rewinding (reverse branch migration). Consistent with this idea, *in vitro* studies demonstrate that Top3 specifically recognizes the complex of Sgs1 bound to its DNA substrate (Harmon *et al.* 1999, 2003) and our data suggest that Top3 and Pif1 compete for the same substrate (Figure 3). Since we find no evidence for direct protein–protein interaction between Sgs1 and Pif1 by two-hybrid analysis (unpublished), we favor the idea that Pif1 specifically recognizes and actively rewinds the DNA structure created by Sgs1. *In vitro* studies of possible mechanistic interactions between Pif1 and Sgs1 are needed to further elucidate this interesting genetic interaction that is apparent only in *top3* mutant backgrounds.

We thank Ralph Keil, Robert Reid, Qi Feng, Justin Weinstein, and Hui Zou for plasmids and yeast strains. We thank Brent Wells for technical assistance with the screen for gene dosage suppressors of

top3-ts and analysis of Rrm3 localization. We are grateful to Marco Foiani, Peter Thorpe, Michael Lisby, Erika Shor, and Robert Reid for critical reading of the manuscript. This work was supported by National Cancer Institute National Research Service Award grant CA90047 to M.W. and National Institutes of Health grant GM50237 to R.R.

LITERATURE CITED

Akada, R., J. Yamamoto and I. Yamashita, 1997 Screening and identification of yeast sequences that cause growth inhibition when overexpressed. Mol. Gen. Genet. **254:** 267–274.

Aravind, L., D. R. Walker and E. V. Koonin, 1999 Conserved domains in DNA repair proteins and evolution of repair systems. Nucleic Acids Res. **27:** 1223–1242.

Bachrati, C. Z., and I. D. Hickson, 2003 RecQ helicases: suppressors of tumorigenesis and premature aging. Biochem. J. **374:** 577–606.

Bennett, R. J., J. L. Keck and J. C. Wang, 1999 Binding specificity determines polarity of DNA unwinding by the Sgs1 protein of *Saccharomyces cerevisiae*. J. Mol. Biol. **289:** 235–248.

Bennett, R. J., M. F. Noirot-Gros and J. C. Wang, 2000 Interaction between yeast *sgs1* helicase and DNA topoisomerase III. J. Biol. Chem. **275:** 26898–26905.

Bennett, R. J., J. A. Sharp and J. C. Wang, 1998 Purification and characterization of the Sgs1 DNA helicase activity of *Saccharomyces cerevisiae*. J. Biol. Chem. **273:** 9644–9650.

Bennett, R. J., and J. C. Wang, 2001 Association of yeast DNA topoisomerase III and Sgs1 DNA helicase: studies of fusion proteins. Proc. Natl. Acad. Sci. USA **98:** 11108–11113.

Bessler, J. B., J. Z. Torredagger and V. A. Zakian, 2001 The Pif1p subfamily of helicases: Region-specific DNA helicases? Trends Cell. Biol. **11:** 60–65.

Bevis, B. J., and B. S. Glick, 2002 Rapidly maturing variants of the Discosoma red fluorescent protein (DsRed). Nat. Biotechnol. **20:** 83–87.

Brachmann, C. B., A. Davies, G. J. Cost, E. Caputo, J. Li *et al.*, 1998 Designer deletion strains derived from *Saccharomyces cerevisiae* S288C: a useful set of strains and plasmids for PCR-mediated gene disruption and other applications. Yeast **14:** 115–132.

Chakraverty, R. K., J. M. Kearsey, T. J. Oakley, M. Grenon, M. A. de La Torre Ruiz *et al.*, 2001 Topoisomerase III acts upstream of Rad53p in the S-phase DNA damage checkpoint. Mol. Cell. Biol. **21:** 7150–7162.

Champoux, J. J., 2001 DNA topoisomerases: structure, function, and mechanism. Annu. Rev. Biochem. **70:** 369–413.

Christianson, T. W., R. S. Sikorski, M. Dante, J. H. Shero and P. Hieter, 1992 Multifunctional yeast high-copy-number shuttle vectors. Gene **110:** 119–122.

Cobb, J. A., L. Bjergbaek, K. Shimada, C. Frei and S. M. Gasser, 2003 DNA polymerase stabilization at stalled replication forks requires Mec1 and the RecQ helicase Sgs1. EMBO J. **22:** 4325–4336.

Constantinou, A., M. Tarsounas, J. K. Karow, R. M. Brosh, V. A. Bohr *et al.*, 2000 Werner's syndrome protein (WRN) migrates Holliday junctions and co-localizes with RPA upon replication arrest. EMBO Rep. **1:** 80–84.

Cross, F. R., 1997 'Marker swap' plasmids: convenient tools for budding yeast molecular genetics. Yeast **13:** 647–653.

Declais, A. C., J. Marsault, F. Confalonieri, C. B. de La Tour and M. Duguet, 2000 Reverse gyrase, the two domains intimately cooperate to promote positive supercoiling. J. Biol. Chem. **275:** 19498–19504.

DiGate, R. J., and K. J. Marians, 1988 Identification of a potent decatenating enzyme from *Escherichia coli*. J. Biol. Chem. **263:** 13366–13373.

Doe, C. L., J. Dixon, F. Osman and M. C. Whitby, 2000 Partial suppression of the fission yeast *rqh1(−)* phenotype by expression of a bacterial Holliday junction resolvase. EMBO J. **19:** 2751–2762.

Duguet, M., 1997 When helicase and topoisomerase meet! J. Cell Sci. **110:** 1345–1350.

Duguet, M., C. Jaxel, A. C. Declais, F. Confalonieri, J. Marsault *et al.*, 2001 Analyzing reverse gyrase activity. Methods Mol. Biol. **95:** 35–49.

Duno, M., B. Thomsen, O. Westergaard, L. Krejci and C. Bendixen, 2000 Genetic analysis of the *Saccharomyces cerevisiae* Sgs1 helicase defines an essential function for the Sgs1–Top3 complex in the absence of *SRS2* or *TOP1*. Mol. Gen. Genet. **264:** 89–97.

Erdeniz, N., U. H. Mortensen and R. Rothstein, 1997 Cloning-free PCR-based allele replacement methods. Genome Res. **7:** 1174–1183.

Fricke, W. M., V. Kaliraman and S. J. Brill, 2001 Mapping the DNA topoisomerase III binding domain of the Sgs1 DNA helicase. J. Biol. Chem. **276:** 8848–8855.

Gangloff, S., B. de Massy, L. Arthur, R. Rothstein and F. Fabre, 1999 The essential role of yeast topoisomerase III in meiosis depends on recombination. EMBO J. **18:** 1701–1711.

Gangloff, S., M. R. Lieber and R. Rothstein, 1994a Transcription, topoisomerases and recombination. Experientia **50:** 261–269.

Gangloff, S., J. P. McDonald, C. Bendixen, L. Arthur and R. Rothstein, 1994b The yeast type I topoisomerase Top3 interacts with Sgs1, a DNA helicase homolog: a potential eukaryotic reverse gyrase. Mol. Cell. Biol. **14:** 8391–8398.

Gietz, R. D., and R. A. Woods, 2002 Transformation of yeast by lithium acetate/single-stranded carrier DNA/polyethylene glycol method. Methods Enzymol. **350:** 87–96.

Goodwin, A., S. W. Wang, T. Toda, C. Norbury and I. D. Hickson, 1999 Topoisomerase III is essential for accurate nuclear division in *Schizosaccharomyces pombe*. Nucleic Acids Res. **27:** 4050–4058.

Gorbalenya, A. E., and E. V. Koonin, 1993 Helicases: amino acid sequence comparisons and structure-function relationships. Curr. Opin. Struct. Biol. **3:** 419–429.

Harmon, F. G., J. P. Brockman and S. C. Kowalczykowski, 2003 RecQ helicase stimulates both DNA catenation and changes in DNA topology by topoisomerase III. J. Biol. Chem. **278:** 42668–42678.

Harmon, F. G., R. J. DiGate and S. C. Kowalczykowski, 1999 RecQ helicase and topoisomerase III comprise a novel DNA strand passage function: a conserved mechanism for control of DNA recombination. Mol. Cell **3:** 611–620.

Harmon, F. G., and S. C. Kowalczykowski, 1998 RecQ helicase, in concert with RecA and SSB proteins, initiates and disrupts DNA recombination. Genes Dev. **12:** 1134–1144.

Heyer, W. D., K. T. Ehmsen and J. A. Solinger, 2003 Holliday junctions in the eukaryotic nucleus: Resolution in sight? Trends Biochem. Sci. **28:** 548–557.

Hudson, Jr., J. R., E. P. Dawson, K. L. Rushing, C. H. Jackson, D. Lockshon *et al.*, 1997 The complete set of predicted genes from *Saccharomyces cerevisiae* in a readily usable form. Genome Res. **7:** 1169–1173.

Ira, G., A. Malkova, G. Liberi, M. Foiani and J. E. Haber, 2003 Srs2 and Sgs1–Top3 suppress crossovers during double-strand break repair in yeast. Cell **115:** 401–411.

Ivessa, A. S., J. Q. Zhou and V. A. Zakian, 2000 The *Saccharomyces* Pif1p DNA helicase and the highly related Rrm3p have opposite effects on replication fork progression in ribosomal DNA. Cell **100:** 479–489.

Karow, J. K., A. Constantinou, J. L. Li, S. C. West and I. D. Hickson, 2000 The Bloom's syndrome gene product promotes branch migration of Holliday junctions. Proc. Natl. Acad. Sci. USA **97:** 6504–6508.

Keil, R. L., and A. D. McWilliams, 1993 A gene with specific and global effects on recombination of sequences from tandemly repeated genes in *Saccharomyces cerevisiae*. Genetics **135:** 711–718.

Kim, R. A., and J. C. Wang, 1992 Identification of the yeast *TOP3* gene product as a single strand-specific DNA topoisomerase. J. Biol. Chem. **267:** 17178–17185.

Klapholz, S., and R. E. Esposito, 1982 A new mapping method employing a meiotic rec-mutant of yeast. Genetics **100:** 387–412.

Krejci, L., S. Van Komen, Y. Li, J. Villemain, M. S. Reddy *et al.*, 2003 DNA helicase Srs2 disrupts the Rad51 presynaptic filament. Nature **423:** 305–309.

Kwan, K. Y., and J. C. Wang, 2001 Mice lacking DNA topoisomerase III beta develop to maturity but show a reduced mean lifespan. Proc. Natl. Acad. Sci. USA **98:** 5717–5721.

Lahaye, A., S. Leterme and F. Foury, 1993 *PIF1* DNA helicase from *Saccharomyces cerevisiae*: biochemical characterization of the enzyme. J. Biol. Chem. **268:** 26155–26161.

Lahaye, A., H. Stahl, D. Thines-Sempoux and F. Foury, 1991 *PIF1*: a DNA helicase in yeast mitochondria. EMBO J. **10:** 997–1007.

Laursen, L. V., E. Ampatzidou, A. H. Andersen and J. M. Murray, 2003 Role for the fission yeast RecQ helicase in DNA repair in G2. Mol. Cell. Biol. **23:** 3692–3705.

Li, W., and J. C. Wang, 1998 Mammalian DNA topoisomerase III alpha is essential in early embryogenesis. Proc. Natl. Acad. Sci. USA **95:** 1010–1013.

Lisby, M., U. H. Mortensen and R. Rothstein, 2003 Colocalization of multiple DNA double-strand breaks at a single Rad52 repair centre. Nat. Cell Biol. **5:** 572–577.

Lisby, M., R. Rothstein and U. H. Mortensen, 2001 Rad52 forms DNA repair and recombination centers during S phase. Proc. Natl. Acad. Sci. USA **98:** 8276–8282.

Lu, J., J. R. Mullen, S. J. Brill, S. Kleff, A. M. Romeo *et al.*, 1996 Human homologues of yeast helicase. Nature **383:** 678–679.

Maftahi, M., C. S. Han, L. D. Langston, J. C. Hope, N. Zigouras *et al.*, 1999 The *top3(+)* gene is essential in *Schizosaccharomyces pombe* and the lethality associated with its loss is caused by Rad12 helicase activity. Nucleic Acids Res. **27:** 4715–4724.

Mangahas, J. L., M. K. Alexander, L. L. Sandell and V. A. Zakian, 2001 Repair of chromosome ends after telomere loss in *Saccharomyces*. Mol. Biol. Cell **12:** 4078–4089.

Mullen, J. R., V. Kaliraman, S. S. Ibrahim and S. J. Brill, 2001 Requirement for three novel protein complexes in the absence of the Sgs1 DNA helicase in *Saccharomyces cerevisiae*. Genetics **157:** 103–118.

Murray, J. M., H. D. Lindsay, C. A. Munday and A. M. Carr, 1997 Role of *Schizosaccharomyces pombe* RecQ homolog, recombination, and checkpoint genes in UV damage tolerance. Mol. Cell. Biol. **17:** 6868–6875.

Myung, K., C. Chen and R. D. Kolodner, 2001 Multiple pathways cooperate in the suppression of genome instability in *Saccharomyces cerevisiae*. Nature **411:** 1073–1076.

Oakley, T. J., A. Goodwin, R. K. Chakraverty and I. D. Hickson, 2002 Inactivation of homologous recombination suppresses defects in topoisomerase III-deficient mutants. DNA Repair **1:** 463–482.

Ooi, S. L., D. D. Shoemaker and J. D. Boeke, 2003 DNA helicase gene interaction network defined using synthetic lethality analyzed by microarray. Nat. Genet. **35:** 277–286.

Reid, R., M. Lisby and R. Rothstein, 2002a Cloning-free genome alterations in *Saccharomyces cerevisiae* using adaptamer-mediated PCR. Methods Enzymol. **350:** 258–277.

Reid, R. J. D., I. Sunjevaric, M. Keddache and R. Rothstein, 2002b Efficient PCR-based gene disruption in *Saccharomyces* strains using intergenic primers. Yeast **19:** 319–328.

Rose, M. D., P. Novick, J. H. Thomas, D. Botstein and G. R. Fink, 1987 A *Saccharomyces cerevisiae* genomic plasmid bank based on a centromere-containing shuttle vector. Gene **60:** 237–243.

Rothstein, R., 1991 Targeting, disruption, replacement, and allele rescue: integrative DNA transformation in yeast. Methods Enzymol. **194:** 281–301.

Rothstein, R., C. Helms and N. Rosenberg, 1987 Concerted deletions and inversions are caused by mitotic recombination between delta sequences in *Saccharomyces cerevisiae*. Mol. Cell. Biol. **7:** 1198–1207.

Saintigny, Y., K. Makienko, C. Swanson, M. J. Emond and R. J. Monnat, Jr., 2002 Homologous recombination resolution defect in Werner syndrome. Mol. Cell. Biol. **22:** 6971–6978.

Schmidt, K. H., and R. D. Kolodner, 2004 Requirement of Rrm3 helicase for repair of spontaneous DNA lesions in cells lacking Srs2 or Sgs1 helicase. Mol. Cell. Biol. **24:** 3213–3226.

Schofield, M. A., R. Agbunag, M. L. Michaels and J. H. Miller, 1992 Cloning and sequencing of *Escherichia coli mut*R shows its identity to *top*B, encoding topoisomerase III. J. Bacteriol. **174:** 5168–5170.

Schulz, V. P., and V. A. Zakian, 1994 The *Saccharomyces PIF1* DNA helicase inhibits telomere elongation and *de novo* telomere formation. Cell **76:** 145–155.

Sherman, F., G. R. Fink and J. B. Hicks, 1986 *Methods in Yeast Genetics*. Cold Spring Harbor Laboratory Press, Cold Spring Harbor, NY.

Shor, E., S. Gangloff, M. Wagner, J. Weinstein, G. Price *et al.*, 2002 Mutations in homologous recombination genes rescue *top3* slow growth in *Saccharomyces cerevisiae*. Genetics **162:** 647–662.

Sikorski, R. S., and P. Hieter, 1989 A system of shuttle vectors and yeast host strains designed for efficient manipulation of DNA in *Saccharomyces cerevisiae*. Genetics **122:** 19–27.

Stewart, E., C. R. Chapman, F. Al-Khodairy, A. M. Carr and T. Enoch, 1997 *rqh1+*, a fission yeast gene related to the Bloom's and Werner's syndrome genes, is required for reversible S phase arrest. EMBO J. **16:** 2682–2692.

Thomas, B. J., and R. Rothstein, 1989 Elevated recombination rates in transcriptionally active DNA. Cell **56:** 619–630.

Tong, A. H., M. Evangelista, A. B. Parsons, H. Xu, G. D. Bader *et al.*, 2001 Systematic genetic analysis with ordered arrays of yeast deletion mutants. Science **294:** 2364–2368.

Torres, J. Z., S. L. Schnakenberg and V. A. Zakian, 2004 *Saccharomyces cerevisiae* Rrm3p DNA helicase promotes genome integrity by preventing replication fork stalling: viability of *rrm3* cells requires the intra-S-phase checkpoint and fork restart activities. Mol. Cell. Biol. **24:** 3198–3212.

Veaute, X., J. Jeusset, C. Soustelle, S. C. Kowalczykowski, E. Le Cam *et al.*, 2003 The Srs2 helicase prevents recombination by disrupting Rad51 nucleoprotein filaments. Nature **423:** 309–312.

Wallis, J. W., G. Chrebet, G. Brodsky, M. Rolfe and R. Rothstein, 1989 A hyper-recombination mutation in *S. cerevisiae* identifies a novel eukaryotic topoisomerase. Cell **58:** 409–419.

Watt, P. M., E. J. Louis, R. H. Borts and I. D. Hickson, 1995 Sgs1: a eukaryotic homolog of *E. coli* RecQ that interacts with topoisomerase II *in vivo* and is required for faithful chromosome segregation. Cell **81:** 253–260.

Winzeler, E. A., D. D. Shoemaker, A. Astromoff, H. Liang, K. Anderson *et al.*, 1999 Functional characterization of the *S. cerevisiae* genome by gene deletion and parallel analysis. Science **285:** 901–906.

Wu, L., S. L. Davies, N. C. Levitt and I. D. Hickson, 2001 Potential role for the *BLM* helicase in recombinational repair via a conserved interaction with *RAD51*. J. Biol. Chem. **276:** 19375–19381.

Wu, L., and I. D. Hickson, 2002 The Bloom's syndrome helicase stimulates the activity of human topoisomerase III alpha. Nucleic Acids Res. **30:** 4823–4829.

Wu, L., and I. D. Hickson, 2003 The Bloom's syndrome helicase suppresses crossing over during homologous recombination. Nature **426:** 870–874.

Wu, L., J. K. Karow and I. D. Hickson, 1999 Genetic recombination: helicases and topoisomerases link up. Curr. Biol. **9:** R518–R520.

Wu, L., K. L. Chan, C. Ralf, D. A. Bernstein, P. L. Garcia *et al.*, 2005 The HRDC domain of BLM is required for the dissolution of double Holliday junctions. EMBO J. **24:** 2679–2687.

Zhou, J., E. K. Monson, S. Teng, V. P. Schulz and V. A. Zakian, 2000 Pif1p helicase, a catalytic inhibitor of telomerase in yeast. Science **289:** 771–774.

Zhu, Q., P. Pongpech and R. J. DiGate, 2001 Type I topoisomerase activity is required for proper chromosomal segregation in *Escherichia coli*. Proc. Natl. Acad. Sci. USA **98:** 9766–9771.

Zou, H., and R. Rothstein, 1997 Holliday junctions accumulate in replication mutants via a RecA homolog-independent mechanism. Cell **90:** 87–96.

Communicating editor: M. Lichten